Quantifying β-catenin subcellular dynamics and cyclin D1 mRNA transcription during Wnt signaling in single living cells

Pinhas Kafri, Sarah E. Hasenson, Itamar Kanter, Jonathan Sheinberger, Noa Kinor, Sharon Yunger, and Yaron Shav-Tal*

The Mina & Everard Goodman Faculty of Life Sciences & Institute of Nanotechnology, Bar-Ilan University, Ramat Gan 52900, Israel

*Correspondence should be addressed to Y.S-T. (e-mail: Yaron.Shav-Tal@biu.ac.il)

ABSTRACT

Signal propagation from the cell membrane to a promoter can induce gene expression. To examine signal transmission through sub-cellular compartments and its effect on transcription levels in individual cells within a population, we used the Wnt/β-catenin signaling pathway as a model system. Wnt signaling orchestrates a response through nuclear accumulation of β-catenin in the cell population. However, quantitative live-cell measurements in individual cells showed variability in nuclear β-catenin accumulation, which could occur in two waves, followed by slow clearance. Nuclear accumulation dynamics were initially rapid, cell cycle independent and differed substantially from LiCl stimulation, presumed to mimic Wnt signaling. β-catenin levels increased simultaneously at adherens junctions and the centrosome, and a membrane-centrosome transport system was revealed. Correlating β-catenin nuclear dynamics to *cyclin D1* transcriptional activation showed that the nuclear accumulation rate of change of the signaling factor, and not actual protein levels, correlated with the transcriptional output of the pathway.

INTRODUCTION

Imaging of gene expression in individual cells using quantitative microscopy has become a central experimental approach for unraveling the dynamic aspects of mRNA transcription[1-3], and for examining various events of gene expression in real time[4-9]. Cells govern specific transcriptional responses to various stimuli by use of signaling pathways and transducing factors that relay the signal to the promoters of induced target genes[10,11]. Studies of transcription factor dynamics in single cells in response to signaling have revealed dynamic aspects of transcription factor nuclear translocation and modulation[12-17]. This study centers on the dynamics of the Wnt/β-catenin signaling pathway and its control of *cyclin D1* gene expression, as a model system for examining the dissemination of a signal in the cell and the transcriptional response it elicits.

The Wnt/β-catenin canonical signaling pathway is activated by the binding of the Wnt ligand to plasma membrane receptors, thereby triggering downstream events that culminate in the accumulation of β-catenin in the cytoplasm and its translocation into the nucleus[18-20]. The interaction of β-catenin with transcription factors of the TCF/LEF family in the nucleus modifies gene expression of crucial genes, thus leading to changes in key cellular pathways, such as proliferation, migration and cell fate[21]. Mechanistically, in the absence of Wnt, cytoplasmic β-catenin protein is constantly degraded[22] via the "destruction complex" and proteosomal degradation[23-25], thus preventing β-catenin nuclear targeting. In many pathological cases β-catenin is not degraded but accumulates in the nucleus and activates genes, some of which are associated with cell proliferation, such as *MYC* and *cyclin D1*[26,27]. The cyclin D1 protein is a major player in the regulation

of the cell cycle[28,29] and its expression is regulated at several levels, including mRNA transcription[30] via an elaborate promoter region[31]. Cyclin D1 levels were shown to be induced by the Wnt/β-catenin canonical signaling pathway[26,27,32-37].

The Wnt/β-catenin signaling pathway has received much experimental attention due to its centrality in gene expression patterning, and its involvement in many cancer types[38]. While the endpoint of β-catenin protein stabilization by Wnt signaling has been well studied biochemically, the kinetic aspects of this signaling pathway in living cells, for the β-catenin protein and the target mRNA, remain under-studied. To address this topic we used a cell system for the *in vivo* visualization and analysis of mammalian mRNA transcriptional kinetics of single alleles[39,40]. Whereas, we had previously followed transcription from a single *cyclin D1* (*CCND1)* gene in living human cells, we now set out to examine the real-time behavior of β-catenin during active signaling in a population of living cells, and the effect of signaling on the activity pattern of the target gene.

RESULTS

System for studying Wnt/β-catenin signaling and gene activation in single living cells

We previously generated a cell system in which a *CCND1* gene was integrated as a single copy allele into human HEK293 cells using Flp-In recombination[39]. Transcription kinetics on this gene were visualized and quantified using RNA FISH and live-cell imaging techniques. RNA tagging was achieved using a series of MS2 sequence repeats[41] inserted into the long 3'UTR of *CCND1*. The MS2 repeats form stem-loop structures in the transcribed mRNA. By co-expressing a fluorescent coat protein termed MS2-CP-GFP that binds to the MS2 stem-loops, we obtained fluorescent tagging of the mRNAs produced from this gene, designated *CCND1-MS2*[39,40]. This *CCND1-MS2* allele is under the regulation of the endogenous *cyclin D1* promoter[42] and therefore serves as a candidate gene for activation by Wnt/β-catenin signaling[43].

Studying individual living cells, we found that the *CCND1-MS2* gene transits between transcriptionally active and non-active states under steady-state conditions[39]. At steady state, only around 40-50% of cells were actively transcribing *CCND1-MS2*. In order to verify that the Wnt signaling pathway activates the *CCND1-MS2* gene we added Wnt3a conditioned medium to the cells and imaged the cells over time. Indeed, on the population level, after 75 min over 80% of cells had shown an actively transcribing *CCND1-MS2* gene (Figure 1a, b, Supplementary file 1a, Video 1).

Since an imaging-based approach for studying signaling dynamics requires that relevant molecules be fluorescently tagged, we verified using a luciferase assay, that a YFP-

tagged version of β-catenin[19] activates the *CCND1* promoter, and observed 2.3 fold activation after transient transfection of the protein into the HEK293 *CCND1-MS2* cells (Figure 1-figure supplement 1a). We note that HEK293 cells are known to have a low background of β-catenin activity[44], and are not known to have mutations in proteins associated with Wnt signaling[45]. Immunofluorescence with an antibody to the endogenous β-catenin protein showed normal β-catenin localization at the cell membrane region (a portion of β-catenin is located in adherens junctions and functions in cell adhesion[46]), as well as low cytoplasmic levels under non-induced conditions, compared to a predominant increase in cytoplasmic and nuclear distribution after the addition of Wnt3a (Figure 1c). In summary, this cell system enables the measurement of *CCND1* transcription activation kinetics in single cells following Wnt signaling.

To mimic endogenous β-catenin distribution using YFP-β-catenin, we generated a HEK293 *CCND1-MS2* cell clone that stably expressed YFP-β-catenin. Since high overexpression conditions of YFP-β-catenin typically result in increased subcellular distribution and high accumulation in the nucleus prior to any signal (Figure 1-figure supplement 1b), which is in stark contrast to the endogenous β-catenin protein that is observed mainly at the membrane (Figure 1c), we screened and identified a clone that stably expressed low levels of YFP-β-catenin. The clone phenotypically resembled endogenous protein localization and distribution, namely, membrane localization in the non-induced state, and enhanced nuclear localization following Wnt stimulation (Figure 1d). Characterization of endogenous β-catenin and YFP-β-catenin accumulation levels by Western blotting showed that YFP-β-catenin expression levels were ~80% of the

endogenous β-catenin, thus doubling β-catenin levels in the cell, and that the accumulation dynamics of both proteins were identical (Figure 1e). The time-scale of β-catenin induction is in agreement with other studies[47,48]. The addition of YFP-β-catenin to the cell clone did not influence the cell cycle or *CCND1* expression at steady state as quantified by single molecule RNA FISH[39,40] (Figure 1-figure supplement 1c-h).

Real-time β-catenin dynamics in a cell population in response to Wnt signaling

To understand the intra-cellular dynamics of β-catenin in a cell population under living cell conditions, cells were imaged for over 12 hours. Rapid nuclear accumulation of β-catenin was observed in most cells that were stimulated with Wnt3a, compared to no change in β-catenin levels in control cells that received mock conditioned medium without Wnt3a (Figure 2a, b, Video 2). Rising levels of β-catenin in the cytoplasm and the nucleus were detected 15 min after Wnt3a addition, and the accumulation peak was observed 2-3 hrs later (Figure 2c), during which β-catenin levels increased 3-fold compared to the initial state. Recombinant Wnt3a (200ng/ml) showed the same dynamics (data not shown). The rate at which β-catenin levels increased in the nucleus was faster than in the cytoplasm, leading to a higher nucleus/cytoplasm (N/C) protein ratio, whereas in the control cells there was no change (Figure 2d).

Analyzing the rate of change in β-catenin levels in the nucleus and cytoplasm over time ($\Delta I/\Delta t$) showed that the accumulation was comprised of two phases; an initial rapid one, in which the peak of the change in accumulation was reached 60 min after induction,

and a second accumulation phase in which cellular β-catenin continued to amass but at a declining rate up until 180 min (Figure 2e). Subsequently, the rate of change turned negative, meaning that β-catenin levels were declining, probably due to degradation. In control cells, the rate of change in β-catenin remained unaltered.

To examine whether the dynamics of nuclear entry of β-catenin were modified during Wnt activation and how they compared to β-catenin shuttling out of the nucleus, we used fluorescence recovery after photobleaching (FRAP). Nuclei of cells showing nuclear β-catenin, either after 2 hrs of Wnt3a activation or transiently overexpressing β-catenin, were photobleached, and nuclear import of β-catenin was monitored over time (Figure 2-figure supplement 1a top). The dynamics were relatively slow, however, the import rate under Wnt3a conditions was more rapid than transient overexpression, showing the advantage of measurements performed at low expression conditions (Figure 2-figure supplement 1a, b, Supplementary file 1b). The incomplete recovery of YFP-β-catenin during the FRAP time-course meant that a significant population of β-catenin molecules had already accumulated and had been retained in the nucleus prior to photobleaching. Next, we photobleached the cytoplasm and found that the rate of β-catenin shuttling out from the nucleus was slower than the import rate (Figure 2-figure supplement 1a bottom, c, Supplementary file 1c). Similarly, fluorescence loss in photobleaching (FLIP), either in the nucleus or in the cytoplasm, showed that β-catenin shuttling out of the nucleus was slower than its nuclear entry (Figure 2-figure supplement 1d, Supplementary file 1d). Altogether, the data suggest that Wnt signaling

causes a transient shift in the dynamic interplay between β-catenin stabilization and degradation processes, towards protein stabilization and accumulation.

Individual cells in the population present a variable response of β-catenin dynamics

The averaged population data obtained from living cells presented above (Figure 2) are in agreement with biochemical data as seen by Western blotting of protein extracts from large cell populations, showing the accumulation of β-catenin beginning from around 30 min after Wnt and peaking at 3 hrs[47,49]. However, the averaged behavior of a population does not necessarily represent the actual dynamics in individual cells. Examining the dynamic behavior of β-catenin accumulation in the nucleus and cytoplasm of individual cells after Wnt3a showed that although an increase in β-catenin levels was initiated in most cells, the subsequent dynamics were variable (Figure 3a, b, Video 3). For instance, comparing cells 1,2 and 4 (Figure 3a) showed a major and rapid wave of β-catenin nuclear accumulation in cell 1 (30-165 min) that subsided and then mildly rose again (465-585 min); a similar range of events occurred in cell 2 but the two waves were less intense and the second wave occurred earlier compared to cell 1 (first wave 30-150 min, second wave 330-435 min); in contrast, cell 4 showed a longer accumulation period (30-240 min). Cells 3 and 6 showed slow nuclear accumulation, peaking late only after 825 min and 525 min, respectively, from Wnt3a stimulation. This analysis showed that the dynamic behavior of β-catenin in the cytoplasm and the nucleus was highly similar within the same cell, but that the time-frames of

accumulation could be quite different between individual cells, some showing 2 cycles of nuclear accumulation. In these cases, the first cycle of accumulation lasted 360 min on average and the second cycle 180 min on average.

The similar dynamics of decline in β-catenin levels in the nucleus and the cytoplasm suggests that β-catenin is not simply shuttling in and out of the nucleus, but rather reflects an enhanced activity of the degradation arm controlling β-catenin levels. To test this, we added lithium chloride (LiCl, 20 mM), a glycogen synthase kinase-3β (GSK3β) inhibitor that mimics Wnt signaling[50,51]. Indeed, LiCl caused β-catenin nuclear and cytoplasmic accumulation, but the dynamics were completely different than Wnt3a (Figure 3-figure supplement 1a, b, and Video 4). β-catenin accumulation occurred synchronously and continuously throughout 10-11 hrs in all cells, and only then did the accumulation cease. The increasing accumulation rate of change ($\Delta I/\Delta t$) in the nucleus and cytoplasm continued for 10 hrs, compared to 3 hrs, in response to Wnt3a (Figure 3-figure supplement 1c, d). The levels of β-catenin were 4-fold higher in LiCl treated cells compared to Wnt3a. Since LiCl prevents β-catenin degradation, we hypothesized that Wnt3a treatment together with the proteasome inhibitor MG132, which stabilizes β-catenin, but not through GSK3β phosphorylation, should have a similar effect on β-catenin dynamics. Indeed, accumulation dynamics under Wnt3a+MG132 were similar to LiCl treatment (Figure 3-figure supplement 1e). Treatment with MG132 without Wnt3a showed the same dynamics (data not shown). When the curve describing the dynamics of β-catenin in response to Wnt3a (Figure 2c) was fitted with a two-phase exponential fit that describes production and degradation (Figure 2-figure supplement 1e), we found

linear accumulation in the first phase, showing that degradation was very low, as expected[47]. β-catenin production rates did not change significantly during the accumulation and clearance phases, whereas, the degradation rate became predominant during the clearance phase. β-catenin degradation had a characteristic time of 2.75 hours. These data exemplify the difference between a signaling molecule and a chemical that target the same signaling pathway. While drug action is less influenced by endogenous molecules, a signaling molecule will relay a transient signaling effect, depending on the level of other signaling molecules that are present in the cell at the time of induction.

Since the maximum levels of β-catenin accumulation differed between cells in the population (Figure 3-figure supplement 2a-e), and we could identify intense and prolonged accumulation in some Wnt3a-treated cells, we examined whether there was a correlation between the time to reach the maximum level and the peak of the response. However, a low correlation score (0.28) was observed for the Wnt3a-treated cells, and a more prominent correlation score (0.53) in LiCl-treated cells (Figure 3-figure supplement 2f, g). The latter was expected due to the continuous accumulation over time. But for Wnt3a treatment, this meant that a longer Wnt3a signaling response did not necessarily result in higher levels of β-catenin accumulation. Moreover, calculating the integral of the fluorescence signal that accumulated over the whole observation period in a cell population (from Figure 3), showed that the total accumulation in most cells was similar (Figure 3-figure supplement 2h), and that differences between single cells were pronounced mainly at earlier time points of the response.

The response of cells to Wnt3a is not cell cycle dependent

Cluster analysis of the dynamic behavior of β-catenin in individual living cells, shows the dramatic difference between Wnt signaling activation by Wnt3a compared to LiCl (Figure 4a; membrane and centrosome will be discussed below). ~80% of the cells showed similar dynamics (e.g. Figure 2c) and ~20% portrayed different behavior patterns (e.g. Figure 3). In order to determine whether the variabilities in β-catenin dynamics in the cell population in response to Wnt3a, may be due to the cell cycle stage, we examined time-lapse movies in which cells had undergone mitosis, and in which daughter cells could be identified. For example, in the population of cells seen accumulating β-catenin in response to Wnt3a in Figure 4b (Video 5), there were two dividing cells at the beginning of the movie, both with low β-catenin levels prior to mitosis. In the daughter cells originating from the top dividing cell there was low β-catenin accumulation, whereas in the bottom dividing cell, one daughter cell responded rapidly and accumulated very high levels of β-catenin, while the other daughter cell responded later and accumulated to low levels (Figure 4 b-e). In summary, we could not detect a pattern of β-catenin accumulation in daughter cells.

To examine the cell cycle and Wnt response more closely in a large population of living cells we used the Fucci system (Video 6 and Video 7), which uses two fluorescent cell cycle markers to identify cell cycle phases[52]. We introduced the Fucci molecules into the CCND1-MS2 cells containing YFP-β-catenin. Cells did not show any special pattern of

YFP-β-catenin accumulation (Figure 4-figure supplement 1a), and cells passing through mitosis also exhibited different accumulation levels in the mother cell and between daughter cells (Figure 4-figure supplement 1b). In summary, we did not identify a cell cycle dependent pattern of YFP-β-catenin levels in response to Wnt.

Wnt signaling induces β-catenin accumulation at the cell membrane and the centrosome

β-catenin is normally present in adherens junctions proximal to the cell membrane, and is bound to E-cadherin in the membrane and to α-catenin, which mediates the connection between the adherens junction and the actin cytoskeleton[53,54]. Not much is known about the subcellular localization of this β-catenin population in response to Wnt. Before treatment, β-catenin was observed as a string of punctate sub-regions distributed along the cell outline only at cell-cell contacts (Figure 3a, Video 3). Since we could detect changes in the intensity of the puncta after Wnt, we followed the intensity of β-catenin at the membrane during Wnt activation and found an increase with similar dynamics to the cytoplasmic and nuclear sub-populations (Figure 5a, Video 8). There was no obvious reduction in the membrane levels even after many hours (Figure 5b). However, the relative increase at the membrane was lower than the nucleus and the cytoplasm, and the rate of β-catenin accumulation ($\Delta I/\Delta t$) at the membrane was less rapid than the nuclear accumulation rates (Figure 5b, c). LiCl caused longer β-catenin

accumulation times and significantly higher accumulation at the membrane (Figure 5c, d).

To examine if Wnt signaling changed the dynamics of β-catenin at the membrane we performed FRAP experiments on this region and found that the recovery dynamics were slow and indicative of slow exchange of β-catenin molecules at the membrane. Yet, similar recovery in unactivated, Wnt3a-treated and LiCl-treated cells was observed, meaning that there was no change in the dynamics of protein exchange but rather an increase in the number of β-catenin molecules in the membrane-bound fraction (Figure 5-figure supplement 1, Supplementary file 1e, f).

In many of the Wnt-induced cells that were followed in the live-cell movies we noticed the appearance of β-catenin in a single prominent dot (Figure 3a, Video 3). β-catenin can localize at the centrosome during interphase and mitosis, and functions in centriolar cohesion[55-57]. Since the β-catenin dot was in proximity to the nucleus, and since the centrosome is juxtaposed to the nucleus, we examined if centrosomal accumulation of β-catenin was occurring. Indeed, movies of dividing cells demonstrated that each daughter cell received one β-catenin-labeled body after division, reminiscent of centrosome behavior (Figure 6a, Video 5 and Video 9). Immunofluorescence of pericentrin (a centrosome marker), together with either endogenous β-catenin or YFP-β-catenin, showed accumulation of β-catenin at the centrosome following activation (Figure 6b).

The accumulation dynamics of β-catenin at the centrosome occurred in parallel to the accumulation seen in the nucleus, cytoplasm and adherens junctions. However, centrosomal levels were significantly high, 5-fold higher compared to the initial state (Figure 6c). The rates of change were the highest and most rapid of all measured cell compartments (Figure 6d). LiCl also led to β-catenin localization at the centrosome, but here too with very different dynamics from Wnt3a (Figure 6d; Figure 3-figure supplement 1f). To obtain a more general outlook of the changes in β-catenin levels in all 4 compartments, we performed a correlation analysis (Figure 6c, e). As was seen in individual cells, the highest correlation in accumulation dynamics following Wnt3a, was observed between the cytoplasm and the nucleus, whereas the lowest correlation was between the centrosome and the membrane.

Interestingly, in some cells we observed β-catenin puncta detaching from the membrane and traveling in the cell (Video 10 and Video 11). When these structures were tracked during movement in the cell, they usually ended up at the centrosome (Figure 6-figure supplement 1). This phenomenon was frequently seen in cells treated with Wnt3a, LiCl and MG132, and less frequently in unactivated cells. We did not observe a correlation with the timing of Wnt addition, and perhaps detection was easier after Wnt due to the increase of β-catenin at the membrane following stimulation. Tracking of the detached β-catenin puncta showed that they reached the centrosome between 30 to 90 min after detachment. To examine whether the residence times of β-catenin molecules at the centrosome resembled the membrane region, we performed FRAP analysis, which showed very rapid recovery kinetics at the centrosome, in

298 comparison to all other cell regions (Figure 6-figure supplement 2). This implied that β-
299 catenin duration at the centrosome is short-lived, with a half-time of fluorescence
300 recovery ($t_{1/2}$) of 1.9 sec, similar to other centrosomal components[58]. Altogether, this
301 suggests that the molecular interactions of β-catenin at the membrane in adherens
302 junctions are significantly more stable than at the centrosome, where the exchange of
303 β-catenin molecules is highly rapid.

304

305 **Wnt signaling modulates the transcriptional output of the *cyclin D1* gene**

306 We next examined the influence of Wnt signaling dynamics on *CCND1* gene activity. As
307 shown (Figure 1a), a significant increase in the percentage of cells actively transcribing
308 CCND1-MS2 could be seen starting 15 min post-activation, and peaking after 75-90 min.
309 Cells returned to steady state activity levels after 6 hrs. We examined several
310 parameters of the transcriptional response. First, we measured the time for an active
311 CCND1-MS2 transcribing gene to appear in the population. In the control unstimulated
312 population (mock conditioned medium), after 120 min most cells had activated the gene
313 once, whereas in Wnt3a-induced cells, gene activation in the population was reached
314 more quickly, already after 60 min. The response time for *CCND1* activation following
315 Wnt3a was also short, ranging at 15 min (Figure 7a-b). This meant that Wnt signaling
316 increased the probability of *CCND1* to initiate transcription.

317 We next examined whether the periods of gene activity were altered after Wnt
318 activation. When *CCND1* was at first non-active and began to transcribe after Wnt3a,

there was prolonged transcriptional activation for a time-frame of 180 min, compared to a shorter activity period of 65 min in unactivated cells (Figure 7c, e, Video 12). This meant that Wnt signaling increased the time-frame of *CCND1* promoter activity. Surprisingly, if the gene was detected in an already active state, and Wnt3a was then added, there was no difference in the activity period compared to that in unactivated cells. Under both conditions, activation persisted for an average of 130 min (Figure 7d), meaning that if the promoter was already activated then there was no Wnt-induced change in this time-frame.

When we examined the levels of CCND1-MS2 activity after Wnt activation in living cells (Figure 8-figure supplement 1a-c), we found that even if the gene was active before Wnt3a addition, the intensity of MS2-GFP fluorescence on the gene showed higher levels, indicative of higher expression levels due to signaling, meaning that the promoter could integrate additional signals (Figure 8-figure supplement 1b). We measured a 1.5-1.7 increase in the maximum MS2-GFP intensity levels, and observed that the maximum intensity distribution for Wnt3a-treated cells shifted such that many more cells displayed higher levels of gene activity (Figure 8a, b, and Figure 8-Figure supplement 1d). The time required to reach the maximum point of activity did not seem to change when examining the whole population (Figure 8-Figure supplement 1e). However, this time was actually shortened from 170 min to 120 min in cells where the gene was initially inactive, and the distribution of cells shifted to shorter times to reach maximum levels of transcription (Figure 8c). This time did not change in cells where the gene was initially active (Figure 8d). When gene activity and gene inactivity patterns were further

examined, not only was an expected increase in the duration of gene activity found, but also a reduction in the rest duration. This means that Wnt activation not only increases the duration time for gene activity, but also reduces periods of inactivity by increasing the frequency of promoter firing events (Figure 7-figure supplement 1).

These measurements suggested that Wnt3a signaling increases promoter firing events so that more CCND1 mRNAs are transcribed. To further examine this on the single mRNA level, we performed quantitative RNA FISH on CCND1-MS2 mRNA molecules in parallel to measuring β-catenin nuclear levels within the same single cell (fixed cells). We counted the number of cellular and nascent CCND1-MS2 mRNAs in Wnt3a-treated cells (Figure 8e) and compared this value to the accumulation levels of nuclear β-catenin in the different cells. Cells that had accumulated β-catenin had significantly higher numbers of cellular CCND1-MS2 mRNAs (3-fold; Figure 8e, f) and nascent CCND1-MS2 mRNAs (3.8-fold; Figure 8e, g, j), which correlated well with the transcription measurements in living cells (Figure 8-figure supplement 1c). Correlating between cellular and nascent CCND1-MS2 mRNA numbers and β-catenin levels showed two sub-populations of high- and low-expressing CCND1-MS2 cells, in correlation with nuclear β-catenin accumulation, respectively (Figure 8h, i). Regarding gene activation, altogether we find that Wnt signaling leads to increased promoter firing frequency, increased gene activity duration time, reduced gene rest time, and significantly higher numbers of mRNAs in the cell.

DISCUSSION

Signaling factors that translocate into the nucleus following signal transduction do so via different modes of shuttling. For instance, some factors display continuous nucleo-cytoplasmic oscillations (p53, mdm2, NF-kB, ERK)[10,12,14,59], while some show a rapid and limited pulse of nuclear build-up (NFAT)[13], or a prolonged presence in the nucleus (MAL)[60]. These dynamics have been characterized using microscopy studies performed in single cells. Biochemical examination of these dynamics can give a true sense of the time-scales of the accumulation as seen by studying protein levels in Western blots[47,48]. However, such approaches cannot provide an accurate temporal dynamic profile of the response as it unfolds within the cell, since they represent an average picture of the behavior of the whole cell population from which the proteins were extracted[61]. By characterizing β-catenin accumulation dynamics in several subcellular compartments within individual living cells, we could examine how varying responses in individual cells translate into a well-timed response of the cell population.

Using a cell system we previously generated to follow CCND1 transcription in real-time on the single gene level[39], we now measured β-catenin sub-cellular dynamics, as well as characterized the transcriptional response of *CCND1* to Wnt. Even though Wnt/β-catenin signaling has been highly studied, the basic propagation dynamics of this signal in single living cells have not been characterized. This is due to the lack of an appropriate system that would allow analysis of the behavior of a fluorescent β-catenin protein that resembles the endogenous protein[62]. Previous studies using transiently overexpressed β-catenin and photobleaching methods were important in establishing

the characteristics of its intra-cellular mobility[19,20]. However, the subcellular distribution of transiently overexpressed fluorescent β-catenin is different than the endogenous protein, since the overexpressed protein is found throughout the whole cell including the nucleus (even without a signal), membrane staining is lacking, and cytoskeletal organization is disrupted[19,20,63]. Even the use of nanobodies targeting endogenous β-catenin in living cells did not mimic the membrane localization of non-induced cells[64]. Hence, using our cell system in which YFP-β-catenin was stably expressed at relatively low levels (80% over the endogenous protein) and was distributed similarly to the endogenous protein, we were able to follow the subcellular dynamics of β-catenin in real-time.

Upon Wnt activation, β-catenin levels in the cell population portrayed a relatively rapid increase in the cells. The general time-scale of hours of β-catenin accumulation concurred with Western blotting experiments[47,48], and altogether portrayed an orchestrated response of the cell population to the Wnt signal. However, examination of the accumulation profiles in single cells showed response patterns deviating from the average behavior in at least 20% of the population; accumulation rates and levels varied, and in some cells additional but less intense waves of β-catenin nuclear accumulation were observed. We suggest that the balance between accumulation and degradation affects the outcome in β-catenin build-up in each cell. The Kirschner group has shown[47] that Wnt does not completely abolish the activity of the destruction complex. We therefore suggest that if the total levels of accumulation are similar in

most cells (e.g. integral analysis), then the level of inhibition of the destruction complex is expected to vary in each cell and to determine the response.

However, the fact that *CCND1* transcriptional activation occurs within the same time frame as the main initial phase of β-catenin nuclear accumulation means that in most cells in the population, the *CCND1* gene will become activated shortly after Wnt activation. Possibly, later phases of β-catenin nuclear accumulation could have an influence on prolonging *CCND1* activity (steady state activity levels return after 6 hrs). Indeed, measurements of *CCND1* activity in living cells following Wnt activation showed a positive change in several parameters relating to gene activation; not only did the frequency of *CCND1* activation in the cell population rise and the time to activate *CCND1* shorten, but the levels of *CCND1* transcriptional output increased, the timeframe of gene activity became substantially longer, and gene resting periods were shortened. Overall, this means that Wnt signaling increases the number of CCND1 mRNAs generated, by increasing the frequency of RNA polymerase II recruitment to the promoter and by lengthening the time of promoter responsiveness. Interestingly, even when an already active *CCND1* gene received the Wnt signal, the levels of gene activity increased.

Although we were unable to examine YFP-β-catenin dynamics and CCND1-MS2 transcription activity simultaneously in living cells, by integrating the measurements of *CCND1* transcriptional activity with the measured dynamics of β-catenin nuclear accumulation from the separate experiments, we found that the rate of change of nuclear β-catenin correlated well with transcription induction (Figure 9a), specifically

during the first rapid phase of nuclear β-catenin accumulation. This fits in well with a previous study demonstrating that the fold change in β-catenin nuclear levels is the element affecting target gene activity[65], and that the transcriptional machinery is capable of computing the fold change in β-catenin, thereby determining the transcriptional response[65]. Similar behavior was observed for the ERK signaling pathway[66]. Hence, it is not the absolute number of β-catenin molecules in the nucleus that correlates with transcription rates, but the rate of change of β-catenin levels over time, and particularly the rapid change during the first phase of induction that elicits the transcriptional effect (Figure 9b). The advantage of such a sensing mechanism would be its ability to buffer out cellular noise and variability in the cell population.

Concurrent β-catenin accumulation the cell membrane and the centrosome were quantified. β-catenin demarcates the cell outline when there are cell-cell contacts due to its presence in adherens junctions[46]. Generally, while the nuclear accumulation of β-catenin has been the focus of Wnt signaling studies, the membrane region has not been considered a major target of the response. However, one study has shown localization of unphosphorylated β-catenin to the membrane upon Wnt activation within 30 min, in cells lacking E-cadherin, although the function was unclear[67]. We found increased β-catenin levels in the membrane following Wnt activation. The punctate membranal pattern persisted during activation, suggesting that Wnt increases the recruitment of β-catenin to existing adherens junctions. Indeed, β-catenin dynamics in the membrane showed a relatively slow exchange both before and after Wnt activation, similar to a study conducted in LiCl induced cells[68]. This implies long residence times of β-catenin in

448 the membrane and that potential binding sites for β-catenin molecules at adherens
449 junctions exist constantly, and only when the protein becomes abundant, do they fill up.

450 Centrosomal localization of β-catenin is known[55-57,69-72]. The exact function is not clear
451 and it probably plays a role in regulation of cell separation. It has been suggested that
452 Wnt signaling abolishes the phosphorylation of β-catenin and leads to centrosome
453 splitting[56]. Our study shows for the first time, the highly rapid accumulation rates of β-
454 catenin at the centrosome in real-time, following Wnt signaling. β-catenin at the
455 centrosome is highly mobile as seen in our FRAP study and in another[57]. Interestingly,
456 we identified a connection between the membranal and centrosomal β-catenin
457 fractions. Puncta of membranal β-catenin were detected moving relatively slowly from
458 the membrane region and ending up at the centrosome, sometimes several in parallel in
459 the same cell. Since unphosphorylated β-catenin is found in the membrane after Wnt[67],
460 we can postulate that the β-catenin fraction moving to the centrosome is
461 unphosporylated, and may be involved in driving cell division.

462 Notably, our study also provides a temporal view of β-catenin dynamics in single cells
463 under conditions of LiCl activation. Although LiCl is considered a chemical that mimics
464 Wnt activation and increases β-catenin levels in the nucleus, it is obvious that the
465 dynamics, build-up rates and levels of β-catenin in all subcellular compartments were
466 dramatically exaggerated and unregulated in comparison to Wnt activation. This should
467 be taken into account when inferring information regarding Wnt signaling and β-catenin
468 from LiCl treatment.

The Wnt pathway has been implicated in cell cycle regulation, and levels of phosporylated β-catenin oscillate and increase towards mitosis[73,74]. Examining cells that had undergone mitosis after Wnt activation, did not show a pattern of β-catenin levels in daughter cells, nor did Fucci labeling uncover a cell cycle pattern of β-catenin accumulation following Wnt. This suggests that Wnt-induced nuclear accumulation is not cell cycle dependent.

The propagation of a signal from a membrane receptor to the gene promoter can follow different types of kinetics. Single-cell analysis revealed significant variability in the dynamics of β-catenin nuclear buildup, but also that most cells did finally accumulate the same total level of β-catenin over time. This behavior is quite different than the serum activation pathway that activates β-actin via MAL shuttling[75]. β-actin transcriptional activation begins less than 5 minutes after serum addition, and β-actin alleles respond in the same manner and same time-frame; i.e. variability of the response in single cells is low. Hence, some signaling cascades must relay the information rapidly and tightly since this will lead to the translation of a highly required protein, e.g. β-actin, to generate a protein that is required for cell motility in response to environmental sensing[76,77]. Other pathways such as Wnt/β-catenin may also signal to activate gene expression, but their response emerges much later, probably since the required biological outcomes, such as cell proliferation, require more regulation points. The changes in β-catenin levels in response to Wnt, in several subcellular compartments, indicate that the signaling pathway does not only activate gene expression but is

490 involved in additional processes. Further studies should reveal the exact roles of these
491 subpopulations of β-catenin in response to signal transduction.

METHODS

Cells and transfections

HEK293 Flp-in CCND1-MS2 cells[39] were maintained in Dulbecco's modified Eagle's medium (DMEM) containing 10% FBS (HyClone Laboratories) and hygromycin selection (100 μg/ml; Sigma). Stable expression of MS2-GFP was obtained by co-transfection of the cells with MS2-GFP (10 μg) and puromycin resistance (300 ng) plasmids using calcium phosphate transfection, and selection with puromycin (1 μg/ml; Invivogen) and hygromycin (100 μg/ml). Stable expression of YFP-β-catenin[19] (10 μg) was performed by calcium phosphate transfection, and selection with neomycin (500 μg/ml; Sigma) and hygromycin (100 μg/ml). Cells with very low expression levels were collected by FACS (FACSAria III, BD Biosciences). Transient expression of YFP-β-catenin was performed using PolyJET (SignaGen).

For generation of Wnt3a conditioned medium (CM) and mock CM, L-Wnt-3A and L-mouse fibroblasts cells were grown in DMEM and 10% FBS, and CM was prepared according to American Tissue Culture Collection (ATCC) instructions[78]. Wnt activation was performed with either Wnts3a-CM or with recombinant human Wnt3a (200 ng/ml; R&D Systems). Wnt3a-CM or mock-CM were added 1:1 to the volume of the cells medium. Cells were also treated with LiCl (20 mM; Sigma) and MG132 (20 μM; Sigma).

The Fucci system (Clontech) was used for cell cycle phase detection. For G1 phase detection, the pRetroX-G1-Red vector (mCherry-hCdt1) was used, and for S/G2/M phase the pRetroX-SG2M-Cyan vector (AmCyan-hGeminin). The Fucci system, being a viral-

based system first required the introduction of the mouse ecotropic retroviral receptor on the membrane surface of HEK293 CCND1-MS2 cells expressing YFP-β-catenin. Transient transfection was performed 24 hours prior to infection using PolyJet transfection with the pBABE ecotropic receptor plasmid (Addgene #10687). This step was performed twice for each infection. After mCherry-hCdt1 infection, mCherry positive cells were collected by FACS and maintained in medium containing puromycin (1 μg/ml; Invivogen). Cells were then transfected with the pBABE ecotropic receptor plasmid and 24 hrs post-transfection, the cells infected with AmCyan-hGeminin. Positive cells were collected by FACS and maintained in medium containing neomycin (500 μg/ml) and puromycin (1 μg/ml). For infections, HEK293T cells were maintained in DMEM containing 10% FBS and used to package the Fucci retroviruses, which were collected over a period of three days before infecting the ecotropic HEK293 cells.

Western blotting

SDS-PAGE and Western blotting were performed as previously described[79]. Primary antibodies used were mouse anti-β-catenin (BD Transduction Laboratories, cat# 610154) and rabbit anti-tubulin (Abcam). The secondary antibody was a HRP-conjugated goat anti-rabbit or anti-mouse IgG (Sigma). Immunoreactive bands were detected by the Enhanced Chemiluminescence kit (ECL, Pierce). Experiments were performed 3 times.

Luciferase assay

HEK293 CCND1-MS2 cells were co-transfected with the cyclin D1 promoter -1745CD1LUC Firefly luciefarse construct[42] and either YFP-β-catenin or eYFP-C1 (mock), together with a *Renilla* luciferase construct using PolyJet transfection. 50 ng of each plasmid were used. A luciferase assay was performed after 24 hrs using the Dual-Glo Luciferase assay system (Promega). After standardization with *Renilla* luciferase activity, a relative luciferase activity was obtained and the mean and standard deviation from triplicate wells was calculated. Each experiment was performed 3 times. YFP-β-catenin[19] was obtained from Jürgen Behrens (University of Erlangen-Nürnberg).

Flow cytometry

Cells were harvested and DNA quantification was performed using 5 μg/ml DAPI solution (Sigma). The BD FACSAria III cell sorter was used. For quantifying DNA in fixed cells, we used a 405nm laser for excitation and a 450/40nm bandpass filter for detection. Data were processed and analyzed using FlowJo software. The average quantification of 3 repeated experiments is presented (mean±s.d).

Immunofluorescence

Cells were grown on coverslips coated by Cell-Tak (BD Biosciences), washed with PBS and fixed for 20 min in 4% PFA. Cells were then permeabilized in 0.5% Triton X-100 for 3

554 min. After blocking, cells were immunostained for 1 hr with a primary antibody, and
555 after subsequent washes the cells were incubated for 1 hr with secondary fluorescent
556 antibodies. Primary antibodies: mouse anti-β-catenin and rabbit anti-pericentrin
557 (Abcam, cat# ab4448). Secondary antibodies: Alexa488-labeled goat anti-mouse IgG and
558 Alexa594-labeled goat anti-rabbit (Invitrogen). Nuclei were counterstained with Hoechst
559 33342 (Sigma) and coverslips were mounted in mounting medium.

560

561 **Fluorescence *in situ* hybridization**

562 CCND1-MS2 cells were grown on coverslips coated by Cell-Tak (BD Biosciences) and
563 fixed for 20 min in 4% paraformaldehyde, and overnight with 70% ethanol at 4°C. The
564 next day cells were washed with 1x PBS and treated for 2.5 min with 0.5% Triton X-100.
565 Cells were washed with 1x PBS and incubated for 10 min in 40% formamide (4% SSC;
566 Sigma). Cells were hybridized overnight at 37°C in 40% formamide with a specific
567 fluorescently-labeled Cy3 DNA probe (~10 ng probe, 50 mer). The next day, cells were
568 washed twice with 40% formamide for 15 min and then washed for two hours with 1X
569 PBS. Nuclei were counterstained with Hoechst 33342 and coverslips were mounted in
570 mounting medium. The probe for the MS2 binding site was:

571 CTAGGCAATTAGGTACCTTAGGATCTAATGAACCCGGGAATACTGCAGAC.

572

573

mRNA quantification

3D stacks (0.2 μm steps, 76 or 51 planes) of the total volume of the cells were collected from fixed CCND1-MS2 cells. The 3D stacks were deconvolved and the specific signals of mRNAs were identified (Imaris, Bitplane). mRNA identification was performed in comparison to deconvolved stacks from cells not containing the MS2 integration, which therefore served as background levels of nonspecific fluorescence. No mRNAs were identified in control cells. The sum of intensity for each mRNA particle and active alleles was measured in the same cells using Imaris, as previously described[39,40]. The single mRNA intensities were pooled and the frequent value was calculated. The sum of intensity at the transcription site was divided by the frequent value of a single mRNA. This ratio provided the number of mRNAs associated with the transcription unit from the point of the MS2-region and onwards. As mRNAs should be associated with a polymerase, this number should reflect the maximum number of polymerases engaged with this region. Quantification and counting experiments were applied to experiments performed on different days.

Fluorescence microscopy, live-cell imaging and data analysis

Wide-field fluorescence images were obtained using the Cell^R system based on an Olympus IX81 fully motorized inverted microscope (60X PlanApo objective, 1.42 NA) fitted with an Orca-AG CCD camera (Hamamatsu) driven by the Cell^R software. Live-cell imaging was carried out using the Cell^R system with rapid wavelength switching. For

time-lapse imaging, cells were plated on glass-bottomed tissue culture plates (MatTek, Ashland, MA) coated by Cell-Tak (BD Biosciences) in medium containing 10% FBS at 37°C. The microscope is equipped with an incubator that includes temperature and CO_2 control (Life Imaging Services, Reinach, Switzerland). For long-term imaging, several cell positions were chosen and recorded by a motorized stage (Scan IM, Märzhäuser, Wetzlar-Steindorf, Germany). In these experiments, HEK293 Flp-in CCND1-MS2 expressing MS2-GFP cells were imaged in 3D (26 planes per time point) every 15 min, at 0.26 μm steps for 6 hrs. HEK293 Flp-in CCND1-MS2 cells expressing YFP-β-catenin were imaged in 3D (15 planes per time point) at 0.7 μm steps, every 15 min, up to 18 hrs. For presentation of the movies, the 4D image sequences were transformed into a time sequence using the maximum or sum projection options or manually selecting the in-focus plane using the ImageJ software. Time-lapse data was collected from single cells in several fields and on several days until reaching an appropriate sample size, and then all single-cell data were pooled and either averaged and presented as plots, or presented as single cell data.

Tracking and data analysis

The intensity of the active transcription sites labeled with MS2-GFP fluorescence in time-lapse movies were corrected for photobleaching using ImageJ, and the 3D movies were transformed to 2D by choosing the in-focus plane in which the intensity of the transcription site is the highest. Movies were manually tracked and the intensity

measured for each frame (*Is*). Background from another location in the nucleus (*In*) was subtracted for each frame, and the final intensity was calculated using: *I = Is(t) − In(t)* and then normalized to the initial intensity.

Measuring the intensity of the YFP-β-catenin signal in the subcellular compartments was performed manually using ImageJ, and background was subtracted from all measurements. When YFP-β-catenin levels were low, DIC images that were acquired in parallel were used for nucleus detection. For measurements of centrosome intensity, the intensity of the centrosome in each frame (*Ic)* was multiplied by the area occupied by the centrosome (*Ac*): *I = Ic(t) *Ac(t)*. For membrane intensity, a sum projection of the 3D movies was used.

Intensity was normalized either to the initial frame or to the highest intensity measured. Values of the nucleus/cytoplasm (N/C) ratio of YFP-β-catenin were obtained by division of the YFP-β-catenin intensity levels measured. Correlation coefficient values were calculated by comparing the intensity of β-catenin over time between all possible pairs of sub-cellular compartments, from Wnt activation onset. Values of rate of change (ΔI/Δt) in YFP-β-catenin in the sub-cellular compartments over time were obtained by measuring the intensity difference (ΔI) between 2 consecutive time points divided by the time difference (Δt) between the 2 time points:

$$\frac{\Delta I}{\Delta t}_{(t)n+1/2} = \frac{I_{(t)n+1} - I_{(t)n}}{t_{n+1} - t_n}$$

FRAP and FLIP

FRAP and FLIP experiments were performed using a 3D-FRAP system (Photometrics) built on an Olympus IX81 microscope (636 Plan-Apo, 1.4 NA) equipped with an EM-CCD (Quant-EM, Roper), 491nm laser, Lambda DG-4 light source (Sutter), XY&Z stages (Prior), and driven by MetaMorph (Molecular Devices). Experiments were performed at 37°C with 5% CO_2 using a live-cell chamber system (Tokai). For each acquisition, YFP-β-catenin was bleached using the 491 nm laser. Six pre-bleach images were acquired. In FRAP, post-bleach images were acquired every 0.8 sec for 80 sec in the cytoplasm and the nucleus, every 1 sec for 2 min in adherens junctions, every 0.4 sec for 40 sec at the centrosome, and every 1.5 sec for 8 min to measure nuclear import and export rates. In FLIP, images were acquired every 1.9 sec for 280 sec in the cytoplasm and the nucleus. The experiments were analyzed using ImageJ macros previously described [79]. Data from at least 10 experiments for each cell line were collected and the averaged FRAP and FLIP measurements were fitted by Matlab with a double exponential model:

$I(t) = \alpha_1 * \exp(-\tau_1 * t) + \alpha_2 * \exp(-\tau_2 * t) + c$ Where t=0 is the time immediately after photobleaching.

$t_{0.5}$ was defined as time where $I(t = t_{0.5}) = \frac{I(t=\infty)}{2}$.

Modeling β-catenin dynamics

We used a simple model for describing β-catenin concentration (C) dynamics in the nucleus based on the data presented in the plot from Figure 2c:

$$\frac{dC}{dt} = P(t) - \alpha(t)C$$

Where α is the time dependent degradation rate, and P is the time dependent production rate. Both rates are allowed to change when t=T:

$$\alpha(t) = \begin{cases} \alpha_1;\ for\ t \leq T \\ \alpha_2;\ for\ t > T \end{cases}$$

$$P(t) = \begin{cases} P_1;\ for\ t \leq T \\ P_2;\ for\ t > T \end{cases}$$

The solution is:

$$C(t) = \begin{cases} \left[C(0) - \frac{P_1}{\alpha_1}\right] * e^{-\alpha_1 * t} + \frac{P_1}{\alpha_1};\ for\ t \leq T \\ \left[C(T) - \frac{P_2}{\alpha_2}\right] * e^{-\alpha_2 * (t-T)} + \frac{P_2}{\alpha_2};\ for\ t > T \end{cases}$$

Where:

$$C(T) = \left[C(0) - \frac{P_2}{\alpha_1}\right] * e^{-\alpha_1 * t} + \frac{P_2}{\alpha_1}$$

We fit the model by minimizing the sum of the squares of the residuals with the function “fmincon” in MATLAB using the “active-set” algorithm.

Statistical analysis

Two tailed t-test was performed in the following experiments: Quantitative FISH, Luciferase assay, N/C ratio of YFP-β-catenin and live cell analysis. A Mann–Whitney test was performed in FRAP and FLIP experiments (Supplementary file 1).

ACKNOWLEDGEMENTS

We thank Yinon Ben-Neriah (Hebrew University Medical School) for the L-Wnt-3A and L-mouse fibroblasts cells and Jürgen Behrens (University of Erlangen-Nürnberg) for YFP-β-catenin. This work was supported by the European Research Council and the Israel Cancer Research Fund (YST).

AUTHOR CONTRIBUTIONS

PK designed and performed all the experiments. PK and IK analyzed the data. Others assisted in: cell cycle analysis (SH), Fucci infections (JS), Western blotting (NK), cell line generation (SY). YST wrote the paper.

COMPETING FINANCIAL INTERESTS

The authors declare no competing financial interests.

References

1. Darzacq, X, Yao, J, Larson, DR, Causse, SZ, Bosanac, L, de Turris, V, Ruda, VM, Lionnet, T, Zenklusen, D, Guglielmi, B, Tjian, R & Singer, RH. Imaging transcription in living cells. (2009) *Annu Rev Biophys* **38**, 173-96.
2. Coulon, A, Chow, CC, Singer, RH & Larson, DR. Eukaryotic transcriptional dynamics: from single molecules to cell populations. (2013) *Nat Rev Genet* **14**, 572-84.
3. Hager, GL, McNally, JG & Misteli, T. Transcription dynamics. (2009) *Mol Cell* **35**, 741-53.
4. Darzacq, X, Shav-Tal, Y, de Turris, V, Brody, Y, Shenoy, SM, Phair, RD & Singer, RH. In vivo dynamics of RNA polymerase II transcription. (2007) *Nat Struct Mol Biol* **14**, 796-806.
5. Huranova, M, Ivani, I, Benda, A, Poser, I, Brody, Y, Hof, M, Shav-Tal, Y, Neugebauer, KM & Stanek, D. The differential interaction of snRNPs with pre-mRNA reveals splicing kinetics in living cells. (2010) *J Cell Biol* **191**, 75-86.
6. Brody, Y, Neufeld, N, Bieberstein, N, Causse, SZ, Bohnlein, EM, Neugebauer, KM, Darzacq, X & Shav-Tal, Y. The in vivo kinetics of RNA polymerase II elongation during co-transcriptional splicing. (2011) *PLoS Biol* **9**, e1000573.
7. Martins, SB, Rino, J, Carvalho, T, Carvalho, C, Yoshida, M, Klose, JM, de Almeida, SF & Carmo-Fonseca, M. Spliceosome assembly is coupled to RNA polymerase II dynamics at the 3' end of human genes. (2011) *Nat Struct Mol Biol* **18**, 1115-23.
8. Yao, J, Munson, KM, Webb, WW & Lis, JT. Dynamics of heat shock factor association with native gene loci in living cells. (2006) *Nature* **442**, 1050-3.
9. Mueller, F, Mazza, D, Stasevich, TJ & McNally, JG. FRAP and kinetic modeling in the analysis of nuclear protein dynamics: what do we really know? (2010) *Curr Opin Cell Biol* **22**, 403-11.
10. Purvis, JE & Lahav, G. Encoding and Decoding Cellular Information through Signaling Dynamics. (2013) *Cell* **152**, 945-56.
11. Carmo-Fonseca, M, Platani, M & Swedlow, JR. Macromolecular mobility inside the cell nucleus. (2002) *Trends Cell Biol* **12**, 491-5.
12. Kalo, A & Shav-Tal, Y. Acting on impulse: dissecting the dynamics of the NFAT transcriptional response. (2013) *Genome Biol* **14**, 102.

13. Yissachar, N, Sharar Fischler, T, Cohen, AA, Reich-Zeliger, S, Russ, D, Shifrut, E, Porat, Z & Friedman, N. Dynamic Response Diversity of NFAT Isoforms in Individual Living Cells. (2012) *Mol Cell* **49,** 322-30.

14. Lahav, G, Rosenfeld, N, Sigal, A, Geva-Zatorsky, N, Levine, AJ, Elowitz, MB & Alon, U. Dynamics of the p53-Mdm2 feedback loop in individual cells. (2004) *Nat Genet* **36**, 147-50.

15. Loewer, A, Batchelor, E, Gaglia, G & Lahav, G. Basal dynamics of p53 reveal transcriptionally attenuated pulses in cycling cells. (2010) *Cell* **142**, 89-100.

16. Nelson, DE, Ihekwaba, AE, Elliott, M, Johnson, JR, Gibney, CA, Foreman, BE, Nelson, G, See, V, Horton, CA, Spiller, DG, Edwards, SW, McDowell, HP, Unitt, JF, Sullivan, E, Grimley, R, Benson, N, Broomhead, D, Kell, DB & White, MR. Oscillations in NF-kappaB signaling control the dynamics of gene expression. (2004) *Science* **306**, 704-8.

17. Vartiainen, MK, Guettler, S, Larijani, B & Treisman, R. Nuclear actin regulates dynamic subcellular localization and activity of the SRF cofactor MAL. (2007) *Science* **316**, 1749-52.

18. Clevers, H & Nusse, R. Wnt/beta-catenin signaling and disease. (2012) *Cell* **149**, 1192-205.

19. Krieghoff, E, Behrens, J & Mayr, B. Nucleo-cytoplasmic distribution of beta-catenin is regulated by retention. (2006) *J Cell Sci* **119**, 1453-63.

20. Jamieson, C, Sharma, M & Henderson, BR. Regulation of beta-catenin nuclear dynamics by GSK-3beta involves a LEF-1 positive feedback loop. (2011) *Traffic* **12**, 983-99.

21. Cadigan, KM & Waterman, ML. TCF/LEFs and Wnt signaling in the nucleus. (2012) *Cold Spring Harb Perspect Biol* **4**.

22. Stamos, JL & Weis, WI. The beta-catenin destruction complex. (2013) *Cold Spring Harb Perspect Biol* **5**, a007898.

23. Aberle, H, Bauer, A, Stappert, J, Kispert, A & Kemler, R. beta-catenin is a target for the ubiquitin-proteasome pathway. (1997) *EMBO J* **16**, 3797-804.

24. Salomon, D, Sacco, PA, Roy, SG, Simcha, I, Johnson, KR, Wheelock, MJ & Ben-Ze'ev, A. Regulation of beta-catenin levels and localization by overexpression of plakoglobin and inhibition of the ubiquitin-proteasome system. (1997) *J Cell Biol* **139**, 1325-35.

25. Orford, K, Crockett, C, Jensen, JP, Weissman, AM & Byers, SW. Serine phosphorylation-regulated ubiquitination and degradation of beta-catenin. (1997) *J Biol Chem* **272**, 24735-8.

26. Shtutman, M, Zhurinsky, J, Simcha, I, Albanese, C, D'Amico, M, Pestell, R & Ben-Ze'ev, A. The cyclin D1 gene is a target of the beta-catenin/LEF-1 pathway. (1999) *Proc Natl Acad Sci U S A* **96**, 5522-7.

27. Tetsu, O & McCormick, F. Beta-catenin regulates expression of cyclin D1 in colon carcinoma cells. (1999) *Nature* **398**, 422-6.

28. Johnson, DG & Walker, CL. Cyclins and cell cycle checkpoints. (1999) *Annu Rev Pharmacol Toxicol* **39**, 295-312.

29. Sherr, CJ. G1 phase progression: cycling on cue. (1994) *Cell* **79**, 551-5.

30. Hosokawa, Y & Arnold, A. Mechanism of cyclin D1 (CCND1, PRAD1) overexpression in human cancer cells: analysis of allele-specific expression. (1998) *Genes Chromosomes Cancer* **22**, 66-71.

31. Klein, EA & Assoian, RK. Transcriptional regulation of the cyclin D1 gene at a glance. (2008) *J Cell Sci* **121**, 3853-7.

32. Chocarro-Calvo, A, Garcia-Martinez, JM, Ardila-Gonzalez, S, De la Vieja, A & Garcia-Jimenez, C. Glucose-induced beta-catenin acetylation enhances Wnt signaling in cancer. (2013) *Mol Cell* **49**, 474-86.

33. Willert, J, Epping, M, Pollack, JR, Brown, PO & Nusse, R. A transcriptional response to Wnt protein in human embryonic carcinoma cells. (2002) *BMC Dev Biol* **2**, 8.

34. Lin, SY, Xia, W, Wang, JC, Kwong, KY, Spohn, B, Wen, Y, Pestell, RG & Hung, MC. Beta-catenin, a novel prognostic marker for breast cancer: its roles in cyclin D1 expression and cancer progression. (2000) *Proc Natl Acad Sci U S A* **97**, 4262-6.

35. Porfiri, E, Rubinfeld, B, Albert, I, Hovanes, K, Waterman, M & Polakis, P. Induction of a beta-catenin-LEF-1 complex by wnt-1 and transforming mutants of beta-catenin. (1997) *Oncogene* **15**, 2833-9.

36. Yun, MS, Kim, SE, Jeon, SH, Lee, JS & Choi, KY. Both ERK and Wnt/beta-catenin pathways are involved in Wnt3a-induced proliferation. (2005) *J Cell Sci* **118**, 313-22.

37. Torre, C, Benhamouche, S, Mitchell, C, Godard, C, Veber, P, Letourneur, F, Cagnard, N, Jacques, S, Finzi, L, Perret, C & Colnot, S. The transforming growth factor-alpha and

774 cyclin D1 genes are direct targets of beta-catenin signaling in hepatocyte proliferation.
775 (2011) *J Hepatol* **55**, 86-95.
776 38. Klaus, A & Birchmeier, W. Wnt signalling and its impact on development and cancer.
777 (2008) *Nat Rev Cancer* **8**, 387-98.
778 39. Yunger, S, Rosenfeld, L, Garini, Y & Shav-Tal, Y. Single-allele analysis of transcription
779 kinetics in living mammalian cells. (2010) *Nat Methods* **7**, 631-3.
780 40. Yunger, S, Rosenfeld, L, Garini, Y & Shav-Tal, Y. Quantifying the transcriptional output of
781 single alleles in single living mammalian cells. (2013) *Nat Protoc* **8**, 393-408.
782 41. Bertrand, E, Chartrand, P, Schaefer, M, Shenoy, SM, Singer, RH & Long, RM. Localization
783 of ASH1 mRNA particles in living yeast. (1998) *Mol Cell* **2**, 437-45.
784 42. Albanese, C, Johnson, J, Watanabe, G, Eklund, N, Vu, D, Arnold, A & Pestell, RG.
785 Transforming p21ras mutants and c-Ets-2 activate the cyclin D1 promoter through
786 distinguishable regions. (1995) *J Biol Chem* **270**, 23589-97.
787 43. Fu, M, Wang, C, Li, Z, Sakamaki, T & Pestell, RG. Minireview: Cyclin D1: normal and
788 abnormal functions. (2004) *Endocrinology* **145**, 5439-47.
789 44. Kang, YJ, Park, HJ, Chung, HJ, Min, HY, Park, EJ, Lee, MA, Shin, Y & Lee, SK. Wnt/beta-
790 catenin signaling mediates the antitumor activity of magnolol in colorectal cancer cells.
791 (2012) *Mol Pharmacol* **82**, 168-77.
792 45. Tan, CW, Gardiner, BS, Hirokawa, Y, Layton, MJ, Smith, DW & Burgess, AW. Wnt
793 signalling pathway parameters for mammalian cells. (2012) *PLoS One* **7**, e31882.
794 46. Harris, TJ & Tepass, U. Adherens junctions: from molecules to morphogenesis. (2010)
795 *Nat Rev Mol Cell Biol* **11**, 502-14.
796 47. Hernandez, AR, Klein, AM & Kirschner, MW. Kinetic responses of beta-catenin specify
797 the sites of Wnt control. (2012) *Science* **338**, 1337-40.
798 48. Lustig, B, Jerchow, B, Sachs, M, Weiler, S, Pietsch, T, Karsten, U, van de Wetering, M,
799 Clevers, H, Schlag, PM, Birchmeier, W & Behrens, J. Negative feedback loop of Wnt
800 signaling through upregulation of conductin/axin2 in colorectal and liver tumors. (2002)
801 *Mol Cell Biol* **22**, 1184-93.
802 49. Li, VS, Ng, SS, Boersema, PJ, Low, TY, Karthaus, WR, Gerlach, JP, Mohammed, S, Heck,
803 AJ, Maurice, MM, Mahmoudi, T & Clevers, H. Wnt signaling through inhibition of beta-
804 catenin degradation in an intact Axin1 complex. (2012) *Cell* **149**, 1245-56.

50. Klein, PS & Melton, DA. A molecular mechanism for the effect of lithium on development. (1996) *Proc Natl Acad Sci U S A* **93**, 8455-9.
51. Hedgepeth, CM, Conrad, LJ, Zhang, J, Huang, HC, Lee, VM & Klein, PS. Activation of the Wnt signaling pathway: a molecular mechanism for lithium action. (1997) *Dev Biol* **185**, 82-91.
52. Sakaue-Sawano, A, Kurokawa, H, Morimura, T, Hanyu, A, Hama, H, Osawa, H, Kashiwagi, S, Fukami, K, Miyata, T, Miyoshi, H, Imamura, T, Ogawa, M, Masai, H & Miyawaki, A. Visualizing spatiotemporal dynamics of multicellular cell-cycle progression. (2008) *Cell* **132**, 487-98.
53. Yap, AS, Brieher, WM & Gumbiner, BM. Molecular and functional analysis of cadherin-based adherens junctions. (1997) *Annu Rev Cell Dev Biol* **13**, 119-46.
54. Brembeck, FH, Rosario, M & Birchmeier, W. Balancing cell adhesion and Wnt signaling, the key role of beta-catenin. (2006) *Curr Opin Genet Dev* **16**, 51-9.
55. Kaplan, DD, Meigs, TE, Kelly, P & Casey, PJ. Identification of a role for beta-catenin in the establishment of a bipolar mitotic spindle. (2004) *J Biol Chem* **279**, 10829-32.
56. Hadjihannas, MV, Bruckner, M & Behrens, J. Conductin/axin2 and Wnt signalling regulates centrosome cohesion. (2010) *EMBO Rep* **11**, 317-24.
57. Bahmanyar, S, Kaplan, DD, Deluca, JG, Giddings, TH, Jr., O'Toole, ET, Winey, M, Salmon, ED, Casey, PJ, Nelson, WJ & Barth, AI. beta-Catenin is a Nek2 substrate involved in centrosome separation. (2008) *Genes Dev* **22**, 91-105.
58. Hames, RS, Crookes, RE, Straatman, KR, Merdes, A, Hayes, MJ, Faragher, AJ & Fry, AM. Dynamic recruitment of Nek2 kinase to the centrosome involves microtubules, PCM-1, and localized proteasomal degradation. (2005) *Mol Biol Cell* **16**, 1711-24.
59. Shankaran, H, Ippolito, DL, Chrisler, WB, Resat, H, Bollinger, N, Opresko, LK & Wiley, HS. Rapid and sustained nuclear-cytoplasmic ERK oscillations induced by epidermal growth factor. (2009) *Mol Syst Biol* **5**, 332.
60. Cui, Y, Hameed, FM, Yang, B, Lee, K, Pan, CQ, Park, S & Sheetz, M. Cyclic stretching of soft substrates induces spreading and growth. (2015) *Nat Commun* **6**, 6333.
61. Levsky, JM & Singer, RH. Gene expression and the myth of the average cell. (2003) *Trends Cell Biol* **13**, 4-6.
62. Tan, CW, Gardiner, BS, Hirokawa, Y, Smith, DW & Burgess, AW. Analysis of Wnt signaling beta-catenin spatial dynamics in HEK293T cells. (2014) *BMC Syst Biol* **8**, 44.

837 63. Ligon, LA, Karki, S, Tokito, M & Holzbaur, EL. Dynein binds to beta-catenin and may
838 tether microtubules at adherens junctions. (2001) *Nat Cell Biol* **3**, 913-7.
839 64. Traenkle, B, Emele, F, Anton, R, Poetz, O, Haeussler, RS, Maier, J, Kaiser, PD, Scholz, AM,
840 Nueske, S, Buchfellner, A, Romer, T & Rothbauer, U. Monitoring interactions and
841 dynamics of endogenous beta-catenin with intracellular nanobodies in living cells.
842 (2015) *Mol Cell Proteomics* **14**, 707-23.
843 65. Goentoro, L & Kirschner, MW. Evidence that fold-change, and not absolute level, of
844 beta-catenin dictates Wnt signaling. (2009) *Mol Cell* **36**, 872-84.
845 66. Cohen-Saidon, C, Cohen, AA, Sigal, A, Liron, Y & Alon, U. Dynamics and variability of
846 ERK2 response to EGF in individual living cells. (2009) *Mol Cell* **36**, 885-93.
847 67. Hendriksen, J, Jansen, M, Brown, CM, van der Velde, H, van Ham, M, Galjart, N,
848 Offerhaus, GJ, Fagotto, F & Fornerod, M. Plasma membrane recruitment of
849 dephosphorylated beta-catenin upon activation of the Wnt pathway. (2008) *J Cell Sci*
850 **121**, 1793-802.
851 68. Johnson, M, Sharma, M, Jamieson, C, Henderson, JM, Mok, MT, Bendall, L & Henderson,
852 BR. Regulation of beta-catenin trafficking to the membrane in living cells. (2009) *Cell*
853 *Signal* **21**, 339-48.
854 69. Bahmanyar, S, Guiney, EL, Hatch, EM, Nelson, WJ & Barth, AI. Formation of extra
855 centrosomal structures is dependent on beta-catenin. (2010) *J Cell Sci* **123**, 3125-35.
856 70. Mbom, BC, Siemers, KA, Ostrowski, MA, Nelson, WJ & Barth, AI. Nek2 phosphorylates
857 and stabilizes beta-catenin at mitotic centrosomes downstream of Plk1. (2014) *Mol Biol*
858 *Cell* **25**, 977-91.
859 71. Huang, P, Senga, T & Hamaguchi, M. A novel role of phospho-beta-catenin in
860 microtubule regrowth at centrosome. (2007) *Oncogene* **26**, 4357-71.
861 72. Vora, S & Phillips, BT. Centrosome-Associated Degradation Limits beta-Catenin
862 Inheritance by Daughter Cells after Asymmetric Division. (2015) *Curr Biol* **25**, 1005-16.
863 73. Davidson, G & Niehrs, C. Emerging links between CDK cell cycle regulators and Wnt
864 signaling. (2010) *Trends Cell Biol* **20**, 453-60.
865 74. Hadjihannas, MV, Bernkopf, DB, Bruckner, M & Behrens, J. Cell cycle control of
866 Wnt/beta-catenin signalling by conductin/axin2 through CDC20. (2012) *EMBO Rep* **13**,
867 347-54.

75. Kalo, A, Kanter, I, Shraga, A, Sheinberger, J, Tzemach, H, Kinor, N, Singer, RH, Lionnet, T & Shav-Tal, Y. Cellular Levels of Signaling Factors Are Sensed by beta-actin Alleles to Modulate Transcriptional Pulse Intensity. (2015) *Cell Rep* **11**, 419-32.
76. Kislauskis, EH, Zhu, X & Singer, RH. Sequences responsible for intracellular localization of beta-actin messenger RNA also affect cell phenotype. (1994) *J Cell Biol* **127**, 441-51.
77. Latham, VM, Jr., Kislauskis, EH, Singer, RH & Ross, AF. Beta-actin mRNA localization is regulated by signal transduction mechanisms. (1994) *J Cell Biol* **126**, 1211-9.
78. Shibamoto, S, Higano, K, Takada, R, Ito, F, Takeichi, M & Takada, S. Cytoskeletal reorganization by soluble Wnt-3a protein signalling. (1998) *Genes Cells* **3**, 659-70.
79. Aizer, A, Brody, Y, Ler, LW, Sonenberg, N, Singer, RH & Shav-Tal, Y. The dynamics of mammalian P body transport, assembly, and disassembly in vivo. (2008) *Mol Biol Cell* **19**, 4154-66.
80. Golding, I, Paulsson, J, Zawilski, SM & Cox, EC. Real-time kinetics of gene activity in individual bacteria. (2005) *Cell* **123**, 1025-36.

884 **Figure legends**

885

886 **Figure 1**. Cell system for following β-catenin intra-cellular dynamics and *CCND1* transcription in single living
887 cells. (**a**) CCND1-MS2 HEK293 cells stably expressing MS2-GFP-CP were treated with Wnt3a and followed for 6
888 hrs (every 15 min). Several frames from Video 1 are presented. The number of cells exhibiting transcriptionally
889 active CCND1-MS2 genes (green dot in nucleus, white arrow) was counted over time. Scale bar, 10 μm. (**b**)
890 Plots showing the percentage of cells in the population with actively transcribing CCND1-MS2 genes in Wnt3a-
891 treated (red, n=98) and mock treated (blue, n=128) cells. Mean±s.d from 3 fields imaged on different days -
892 see Supplementary file 1a for statistics. (**c**) Immunofluorescence showing that endogenous β-catenin (green) is
893 prominent at the cell membrane in untreated HEK293 cells (top) and accumulates in the cytoplasm and
894 nucleus following activation by Wnt3a for 2 hrs (bottom). Hoechst DNA stain is in blue. (**d**) Similar changes in
895 subcellular distribution following activation are seen in the YFP-β-catenin low-expressing clone. Bar=10 μm. (**e**)
896 Western blot time course of endogenous β-catenin and YFP-β-catenin protein accumulation following either
897 Wnt3a (top) or LiCl (bottom) stimulation. Anti-β-catenin antibody was used for the detection of both β-catenin
898 proteins. Tubulin was used as a loading control. Time 0 is the time point of activator addition. Blots are
899 representative of 3 repeated experiments. The average quantification of 3 repeated experiments is presented
900 in the plots below (mean±s.d). There is no statistical difference between the endogenous and exogenous
901 levels of β-catenin in the two plots.

902

903 **Figure 2**. The dynamics of β-catenin accumulation following Wnt3a activation in cell populations. Frames from
904 live-cell movies (Video 2) showing YFP-β-catenin dynamics in cells treated with (**a**) mock conditioned medium
905 or (**b**) Wnt3a for 12 hrs. Red bordered frames compare between the 0 min and 120 min time points. Bar=20
906 μm. (**c**) The relative average intensity of β-catenin measured in the cytoplasm (n=24) and nucleus (n=31) of

907 cells treated with Wnt3a for 12 hrs, compared to mock-treated control cells (n=13). (**d**) Nucleus to cytoplasm
908 ratio (N/C) of fluorescence intensities over 12 hrs from **c**. The initial ratio was designated as 1. Inset plot shows
909 the statistical significance p values (t test) at each time point between the two treatments over the
910 experiment time course. (**e**) The rate of change in β-catenin levels (ΔI/Δt), during accumulation or degradation,
911 in the cytoplasm and nucleus over time in cells from **c**.

912

913 **Figure 3**. Variability of β-catenin accumulation dynamics following Wnt3a activation in individual cells. (**a**)
914 Frames from time-lapse Video 3 showing YFP-β-catenin accumulation in a population of cells. The YFP signal is
915 pseudo-coloured using ImageJ 'Green Fire Blue' look-up table. White and yellow arrows point to cells in which
916 β-catenin levels increase and decrease twice during the movie. The pink arrow points to centrosomal
917 accumulation. Bar=10 μm. (**b**) β-catenin levels in the nucleus (left) and cytoplasm (right) in individual cells (as
918 numbered in **a**) are plotted in different colors. The grey background plots show the complete set of plots from
919 all the cells. Maximum β-catenin intensity in each cell was normalized to 1.

920

921 **Figure 4**. Variability of β-catenin dynamics in the cell population and during the cell cycle. (**a**) Heat map and
922 cluster analysis of normalized β-catenin accumulation dynamics in sub-cellular compartments following Wnt3a
923 (top, n(nucleus)=31, n(cytoplasm)=24, n(membrane)=21, n(centrosome)=11) or LiCl (bottom, n(nucleus)=18,
924 n(cytoplasm)=17, n(membrane)=9, n(centrosome)=14) treatments. Data were taken from live-cell movies with
925 each column representing one cell, and rows representing time from Wnt addition. Relative levels of β-catenin
926 are depicted from low (green) to high (red). Hierarchical cluster analysis depicted above the plots shows
927 homogenous behavior in LiCl-treated cells and heterogenous behavior in Wnt3a-treated cells. Most cells reach
928 maximal levels of β-catenin within 2-3 hours. (**b**) (Top) Frames from time-lapse Video 5 showing YFP-β-catenin
929 accumulation in a population of cells. The YFP signal is pseudo-colored using the ImageJ 'Fire' look-up table.

930 Boxes denote cells that go through mitosis, and enlargements are shown below. Green arrows point to
931 mother cells, and yellow and white arrows point to the daughter cells. Bar=10 μm. Plots showing the relative
932 intensity levels of YFP-β-catenin in the cytoplasm and nucleus of the (**c**) top and (**d**) bottom daughter cells of
933 each cell division. (**e**) Plot comparing the relative intensity levels in the nuclei of the four daughter cells.

934

935 **Figure 5**. The dynamics of β-catenin accumulation at the membrane following Wnt3a activation. (**a**) Frames
936 from time-lapse Video 8 showing YFP-β-catenin accumulation at the cell membrane. The YFP signal is pseudo-
937 colored using the ImageJ 'Green Fire Blue' look-up table. Bar=10 μm. (**b**) The relative average intensity of β-
938 catenin measured in the membrane (n=21), cytoplasm and nucleus (from Figure 2) of Wnt3a-treated cells. (**c**)
939 The rate of change in β-catenin levels (ΔI/Δt) accumulation or degradation in the membrane, cytoplasm and
940 nucleus over time in Wnt3a- and LiCl-treated cells. (**d**) The relative average intensity of β-catenin measured in
941 the membrane, cytoplasm and nucleus of LiCl-treated cells.

942

943 **Figure 6**. Accumulation of β-catenin at the centrosome after Wnt3a activation. (**a**) Frames from time-lapse
944 Video 9 showing YFP-β-catenin accumulation at the centrosome (white arrowheads) and after cell division.
945 Bar=10 μm. (**b**) The colocalization (white arrowheads) of YFP-β-catenin (top) or endogenous β-catenin
946 (bottom) with the centrosomal marker pericentrin (red immunofluorescence) in untreated and LiCl-treated
947 cells. Hoechst DNA stain is in blue, and DIC in grey. Boxes show enlarged centrosomal areas. Bar=10 μm. (**c**)
948 The relative average intensity of YFP-β-catenin measured in the centrosome (n=11), membrane, cytoplasm
949 and nucleus (from Figures 2 & 5) of Wnt3a-treated cells. Correlation scores (r) between the nucleus (n),
950 cytoplasm (c), membrane (m) and centrosome (ce) YFP-β-catenin levels are presented at the bottom. (**d**) The
951 rate of change in YFP-β-catenin levels (ΔI/Δt) accumulation or degradation in the centrosome, membrane,
952 cytoplasm and nucleus over time in Wnt3a- and LiCl-treated cells. (**e**) Plots of YFP-β-catenin levels in the sub-

cellular compartments of individual cells (from Figure 3). Boxes show the correlation scores (r) between the nucleus (n), cytoplasm (c), membrane (m) and centrosome (ce).

Figure 7. Measuring the transcriptional response of *CCND1-MS2* to Wnt3a activation in living cells. (**a**) The percentage of cells in a population of either mock-treated (blue) or Wnt3a-activated cells (red) showing an active CCND1-MS2 transcribing gene, over time. (**b**) The promoter response time of *CCND1-MS2* activation from the addition of Wnt3a (n=27) or in mock-treated conditions (n=22). In the boxplots, the median is indicated by a red line, the box represents the interquartile range, the whiskers represent the maximum and minimum values, and red dots represent outliers. (P=0.01). (**c, d**) Periods of gene activity measured in mock-treated and Wnt3a-treated cells. Population was divided into cases where the gene was either not transcribing before addition of Wnt3a or mock-treatment ("off", n(Wnt3a)=27, n(Con)=22, P=0.01) or if the gene was already active ("on", n(Wnt3a)=37, n(Con)=52, P=0.77). *P<0.05, n.s. = P>0.05. (**e**) Frames from Video 12 showing the activation of the *CCND1-MS2* gene detected by MS2-GFP mRNA tagging (arrow) following Wnt3a treatment. Bar= 10 μm.

Figure 8. Quantification of CCND1 activity levels following Wnt activation in single fixed and living cells. (**a,b**) Boxplots showing the maximal MS2-GFP intensity levels reached on actively transcribing CCND1-MS2 genes during 6 hrs in Wnt3a-treated and mock-treated (Con) cells, when (**a**) the gene was either not transcribing before addition of Wnt3a or mock-treatment ("off", n(Wnt3a)=27, n(Con)=22, P=0.0001) or (**b**) if the gene was already active ("on", n(Wnt3a)=37, n(Con)=52, P=0.0006). The median is indicated by a red line, the box represents the interquartile range, the whiskers represent the maximum and minimum values, and red dots represent outliers. (**c, d**) Boxplots showing the time required to reach the maximal intensity levels when (**c**) the gene was either not transcribing before addition of Wnt3a ("off", P=0.03) or (**d**) if the gene was already active

("on", *P*=0.42). (**e**) YFP-β-catenin (yellow) together with RNA FISH images obtained with a probe hybridizing to the MS2 region in the 3'UTR of the CCND1-MS2 mRNA (cyan), showing CCND1 nascent mRNAs on active genes (large dots) and cellular mRNAs (small dots) in Wnt3a-treated cells (2 hrs), in comparison to YFP-β-catenin levels. Nuclei are stained with Hoechst (pseudo-colored red). Bottom row is the pseudo-colored YFP signal using the ImageJ 'Royal' look-up table. Cells are numbered. Bar=10 μm. (**f**) Quantification of the number of cellular CCND1-MS2 mRNAs (ordered from low to high) compared to YFP-β-catenin levels. (**g**) Quantification of the number of nascent CCND1-MS2 mRNAs compared to YFP-β-catenin levels. (**h, i**) Correlation analysis between (**h**) the number of cellular CCND1-MS2 mRNAs and YFP-β-catenin levels and (**i**) between the number of nascent CCND1-MS2 mRNAs and YFP-β-catenin levels. Blue dots – subpopulation with low nuclear YFP-β-catenin levels and low numbers of cellular/nascent CCND1-MS2 mRNAs. Red dots – subpopulation with high nuclear YFP-β-catenin levels and high numbers of cellular/nascent CCND1-MS2 mRNAs. Total correlation score between the number of cellular/nascent CCND1-MS2 mRNAs and YFP-β-catenin levels is 0.88 and 0.59, respectively. (**j**) The field from panel **e** demonstrating higher intensity of active CCND1-MS2 genes in cells with high nuclear YFP-β-catenin levels (red arrows) compared to cells with low nuclear YFP-β-catenin levels (yellow arrows). Active genes are pseudo-colored using the ImageJ 'Red Hot' look-up table. The fluorescent signal of the active genes was enhanced using ImageJ 'Spot Enhancing Filter 2D'. This enhancement led to reduced detectability of single mRNAs in this presentation of the image, in order to emphasize the difference in transcriptional activity between low and high levels of nuclear YFP-β-catenin. Bar=10 μm.

Figure 9. Comparing the kinetics of CCND1 transcriptional activation to the dynamics of β-catenin nuclear accumulation rate of change following Wnt signaling in living cells. (**a**) Plots of the average transcriptional activation kinetics of CCND1-MS2 (red) following Wnt3a activation, compared to the plot of rate of change in β-catenin nuclear accumulation (green). (**b**) Scheme of the dynamic changes occurring in the studied cell system following Wnt signaling. Top - from left to right: Levels of β-catenin (yellow) in the nucleus are

normally low but after addition of Wnt3a to the medium a significant and rapid increase in the nucleus is observed, peaking after 2-3 hrs. β-catenin levels later decline in the nucleus and cytoplasm due to degradation. While this is the average behavior in the population (e.g. cells 1 and 2), when examining individual cells, different dynamics such as multiple pulsations (e.g. cell 3) and rapid initial accumulation (e.g. cell 4) are observed. β-catenin levels increase simultaneously at the membrane and at the centrosome. Bottom- β-catenin induces cyclin D1 transcriptional activity (green dot), and modulation of transcriptional reaction can be observed as the gene reaches higher levels of activity, for longer periods of time. The rate of change in β-catenin accumulation (blue curve, top), rather than the actual levels of β-catenin in the nucleus, correlate with the kinetics of transcriptional activation.

Supplementary Figure legends

Figure 1-figure supplement 1. Measuring the effect of YFP-β-catenin expression in HEK293 cells. (**a**) Luciferase assay showing the levels of cyclin D1 promoter activation following the transient transfection of YFP-β-catenin into HEK293 cells. *P*=0.003. (**b**) Overexpression of YFP-β-catenin shows that overexpressed protein localization does not resemble endogenous β-catenin under non-activated conditions, since it is highly present in the nucleus prior to Wnt activation, and does not appear at the membrane. Bar= 10 μm. (**c**) Cell cycle analysis of HEK293 CCND1-MS2 cells with and without YFP-β-catenin. (**d**) Quantification of CCND1-MS2 nascent mRNAs (left) (*P*=0.8) and cellular mRNAs (right) *(P*=0.16) levels by RNA FISH in HEK293 CCND1-MS2 cell clones with or without YFP-β-catenin (n=18, n=26 respectively). ***P*<0.01, n.s. = *P*>0.05. (**e-h**) Example of single molecule mRNA FISH quantification procedure with a probe that hybridizes to the MS2 region in the 3'UTR of the CCND1-MS2 mRNA. (**e**) Raw 3D image (76 planes in z stack) showing the active transcription site (red) and single mRNA molecules. Hoechst DNA stain is in blue. (**f**) Deconvolved 3D image. Boxes show the transcription

site (bottom) and single cellular mRNAs (top). (**g**) Identification of "spots" of single mRNAs and transcription site (green dots) by Imaris. (**h**) Generation of a 3D shell for each spot to be taken for intensity measurements. Bar= 10 µm. Then the sum of intensity at the transcription site was divided by the frequent intensity value of a single mRNA. This ratio provided the number of mRNAs associated with the transcription unit, as explained in the Methods section.

Figure 2-figure supplement 1. FRAP and FLIP measurements of YFP-β-catenin import and export dynamics. (**a**) Frames showing one pre-bleach frame, the bleach of the YFP-β-catenin in the nucleus (top) or cytoplasm (bottom) of a Wnt3a-treated cell (2 hrs, arrows point to bleached region), and frames following the recovery of signal over time (frame every 1.5 sec for 8 min). Bar=10 µm. (**b**) Averaged data plot of FRAP recovery import curves from Wnt3a-treated cells (n=27, red curve), and transiently overexpressing YFP-β-catenin cells (n=33, blue curve). Pink curve shows the decline in YFP-β-catenin in the cytoplasm of Wnt3-treated cells concurrent with nuclear import (red curve). (**c**) Averaged data plot of FRAP recovery export curves (green) from Wnt3a-treated cells (n=14), compared to the import curve (red). (**d**) FLIP curves for Wnt3a-treated cells photobleached continuously in the nucleus to show import rates from the cytoplasm (n=15, red curve) compared with cells photobleached continuously in the cytoplasm to show export rates from the nucleus (n=16, blue curve). Statistics can be found in Supplementary File 1. (**e**) Data from Figure 2c (blue dots) of nuclear YFP-β-catenin accumulation were fit with a two-phase exponential (red curve).

Figure 3-figure supplement 1. β-catenin accumulation dynamics in response to LiCl activation in individual cells. (**a**) Frames from time-lapse Video 4 showing YFP-β-catenin accumulation in a population of cells. The YFP signal is pseudo-colored using the ImageJ 'Green Fire Blue' look-up table. Bar=10 µm. (**b**) β-catenin levels in the nucleus (top) and cytoplasm (bottom) of individual cells (as numbered in **a**) are plotted in different colors.

The grey background plots show the complete set of plots from all the cells. The maximum intensity of β-catenin in each cell was normalized to 1. (**c**) The relative average intensity of β-catenin measured in the cytoplasm (n=17) and nucleus (n=18) of individual cells treated with LiCl for 12 hrs, compared to Wnt3a-treated cells (from Figure 2). (**d**) The rate of change in β-catenin levels (ΔI/Δt) accumulation or degradation in the cytoplasm and nucleus over time in cells from **c**. (**e**) Frames from a time-lapse movie showing YFP-β-catenin accumulation in a population of Wnt3a+MG132-treated cells. The YFP signal is pseudo-colored using the ImageJ 'Green Fire Blue' look-up table. Bar=10 μm. (**f**) The relative average intensity of β-catenin measured in the centrosome, membrane, cytoplasm and nucleus of LiCl-treated cells.

Figure 3-figure supplement 2. The relationship between YFP-β-catenin levels of accumulation and time of Wnt3a activation. (**a**) Frames from a time-lapse movie showing YFP-β-catenin accumulation in a population of cells in the field. The YFP signal is pseudo-colored using the ImageJ 'Royal' look-up table. Red arrows point to cells with very high β-catenin levels. Bar=10 μm. Plots showing the relative maximal levels of β-catenin measured in nuclei of (**b**) Wnt3a-treated (n=31) or (**c**) LiCl-treated cells (n=18). Order of cells is according to increasing relative intensities. Plots showing the time from the addition of the activator until reaching the maximal levels of β-catenin in the same set of (**d**) Wnt3a-treated or (**e**) LiCl-treated cells. (**f,g**) The respective correlation plots and scores for a Pearson correlation analysis between the maximum intensity in each cell and the time to reach the highest accumulation. (**h**) The integral of the fluorescence values in the 6 cells (from figure 3) showing the total accumulation levels over time during the whole observation period (left). The right-hand plot shows the differences between accumulation in the cells at earlier times.

Figure 4-figure supplement 1. YFP-β-catenin dynamics during the cell cycle in Wnt3a induced cells. HEK293 CCND1-MS2 YFP-β-catenin cells were stably infected with the Fucci system (mCherry-Cdt1 and AmCyan1-

Geminin). Cdt1 levels peak during G1 (red cells), and as cells transition into S, Cdt1 levels decline and Geminin levels rise (cyan cells), remaining high from G2 onwards. (**a**) Frames from Video 6. Before Wnt3a treatment (time 0 min), β-catenin levels are low in the cytoplasm and nucleus of all cells marked by arrowheads (cells in G1 or G2). At time 255 min after Wnt3a, the cells marked with blue, green and pink arrowheads show an increase in the β-catenin levels in response to Wnt signaling. The cell marked with a white arrowhead has not responded yet. At time 780 min, the cell marked with a pink arrowhead has gone through mitosis and the three cells marked by blue, green and white arrowheads have similar β-catenin levels. At time 1065 min, cells marked by white and blue arrowheads are increasing further, while the cell marked with the green arrowhead is not changing. (**b**) Frames from Video 7. Before Wnt3a treatment (time 0 min), all the cells marked with arrowheads (green, blue, white and pink) are in G2. At time 240 min after Wnt3a, the cell marked by a green arrowhead has gone through mitosis and the daughter cells have similar β-catenin levels. At time 420 min, all four cells have gone through mitosis. β-catenin levels in each of the two daughter cells in all four cases are similar to each other. At time 705 min, the daughter cells marked by blue, green and pink arrowheads are different from each other. The cells marked with white arrowheads have similar levels. Bottom rows are the same frames without Fucci labels. Bar=10 μm.

Figure 5-figure supplement 1. FRAP measurements of YFP-β-catenin dynamics at adherens junctions. (**a**) Frames showing one pre-bleach frame, the bleach of the YFP-β-catenin in the membrane region of a Wnt3a-treated cell, and frames following the recovery of signal over time. Circle denotes the bleached region. Bar=10 μm**.** (**b**) Averaged data plot of FRAP recovery curves from mock-treated (control, n=21), Wnt3a-treated (n=32) and LiCl-treated cells (n=18). Statistics can be found in Supplementary file 1e, f.

Figure 6-figure supplement 1. Detachment of membranal YFP-β-catenin puncta and movement towards the centrosome. (**a**) Frames from Video 10 showing the tracks of several YFP-β-catenin membranal puncta (colored tracks) moving from the membrane region towards the centrosome area (red circle). Time is minutes after addition of Wnt3a. YFP signal is shown in negative greyscale colors. Bar=10 μm. (**b**) Maximum time projections of movements of membranal YFP-β-catenin puncta (arrows) towards the centrosome region (circles) in four different cells. The YFP signal is pseudo-colored using the ImageJ 'Green Fire Blue' look-up table. Top row are Wnt3a-treated cells. Bottom row are Wnt3a + MG132-treated cells. Bar=10 μm.

Figure 6-figure supplement 2. Summary of FRAP measurements of YFP-β-catenin dynamics in subcellular compartments in response to Wnt3a treatment. (**a**) Frames showing one pre-bleach frame, the bleach of the YFP-β-catenin in the centrosome of a Wnt3a-treated cell, and frames following the recovery of signal over time. Circle denotes the bleached region. Bar=10 μm. (**b**) Averaged data plot of FRAP recovery curves in the cytoplasm (n=24), nucleus (n=25), membrane (n=32) and centrosome (n=13). Membrane recovery from **Figure 5-figure supplement 1** and import rate to nucleus from **Figure 2-figure supplement 1** are also plotted.

Figure 7-figure supplement 1. Wnt signaling causes shorter rest duration in addition to an increase in the gene burst duration. Plots of single cells demonstrate the active (blue) and inactive (red) state of CCND1-MS2 transcribing gene along 6 hrs in (**a**) mock-treated cells (Control, n=74) and (**b**) Wnt3a-treated cells (n=64). Data were taken from live-cell movies with each column representing one cell along 6 hrs. Histograms showing the distribution of (**c**) active and (**d**) inactive state durations in Wnt3a-treated and mock-treated (Control) cells (*P*=0.02, *P*=0.0004 respectively). The curves are a fit to exponential distribution[80].

Figure 8-figure supplement 1. Transcription site intensity levels in living cells following Wnt3a activation. Plots showing the MS2-GFP average intensity levels measured on active CCND1-MS2 transcription sites during 6 hrs in Wnt3a-treated and in mock-treated cells, when (**a**) the gene was either not transcribing before addition of Wnt3a or mock-treatment ("off", n(Wnt3a)=27, n(Con)=22) (y axis is "relative intensity" going from an "off" state to an "on" state") or (**b**) if the gene was already active to begin with ("on", n(Wnt3a)=37, n(Con)=52) (y axis is the fold change compared to the beginning of the movie). Results were normalized to the intensity at time 0. (**c**) Combined data from **a** and **b**. (**d**) Boxplot (left) showing the MS2-GFP maximal intensity levels reached on active CCND1-MS2 transcription sites during 6 hrs in Wnt3a-treated and in mock-treated cells. In the boxplots, the median is indicated by a red line, the box represents the interquartile range, the whiskers represent the maximum and minimum values, and red dots represent outliers. The histograms (right) show the distribution of maximal intensity levels in these cells (combined data from Figure. 8a and Figure 8b (P=2.13e-06)). The histograms show normalized data such that the area of each bar is relative to the number of observations (i.e. graph height is the probability density of the bar value, and graph area is equal to the probability of obtaining the bar value). The sum area of all bars is 1. The data was fitted with a Gaussian curve. (**e**) Boxplot (left) showing the time required to reach the maximal intensity in Wnt3a-treated and in mock-treated cells. The histograms showing the distribution of this time in these cells (combined data from Figure 8c and Figure 8d, P=0.69). ***P<0.001, n.s. = P>0.05.

Supplemental File 1

Statistical analysis performed in this study. (**a**) The statistical significance p values (t test) at each time point for the percentage of cells showing an active CCND1-MS2 gene (refers to **Figure 1b**) between control and Wnt3a-treated cells. (**b-f**) Mann-Whitney test for comparison between two independent FRAP/FLIP experiments. A statistical comparison between all datasets of two individual FRAP/FLIP experiments are depicted in each plot and are illustrated as a single red circle which marks the p-value (y axis) for all intensity values measured for each time point (x axis). The top and bottom dotted lines indicate where p-value equals 0.05. (**b**) Statistically significant difference between the FRAP dynamics of YFP-β-catenin in the nucleus under Wnt3a treatment versus overexpression of YFP-β-catenin that enters the nucleus without signal, and (**c**) between the FRAP and (**d**) FLIP import and export dynamics (refers to **Figure 2-figure supplement 1**). (**e**) No statistically significant difference between YFP-β-catenin at the cell membrane between mock-treated and Wnt3a-treated cells (refers to **Figure 5-figure supplement 1**). (**f**) No statistically significant difference between YFP-β-catenin at the cell membrane between mock-treated and LiCl-treated cells (refers to **Figure 5-figure supplement 1**).

Supplemental Movies

Video 1. Transcriptional activation of CCND1 in response to Wnt3a. HEK293 CCND1-MS2 cells stably expressing MS2-GFP (green) were treated with Wnt3a. The transcribed CCND1 mRNA on the active gene is seen as a bright green dot. The fluorescent signal on the active genes was enhanced using ImageJ 'Spot Enhancing Filter 2D' in order to clearly present the active sites in the movie. Cells were imaged every 15 min for 3 hrs.

Video 2. YFP-β-catenin dynamics at steady state and after Wnt3a activation. HEK293 CCND1-MS2 cells stably expressing YFP-β-catenin were treated with Wnt3a (top) and showed nuclear and cytoplasmic accumulation of YFP-β-catenin, followed by slow egress. No change in YFP-β-catenin levels was seen in mock-treated cells (bottom). Right – The YFP signal is pseudo-colored using ImageJ 'Royal' look-up table to show YFP-β-catenin levels. Cells were imaged every 15 min for 510 min.

Video 3. YFP-β-catenin dynamics in individual cells. HEK293 CCND1-MS2 cells stably expressing YFP-β-catenin were treated with Wnt3a, and the dynamics of the protein were observed in individual cells. The YFP signal is pseudo-colored using ImageJ ''Green Fire Blue' look-up table to show YFP-β-catenin levels. Cells were imaged every 15 min for 825 min.

Video 4. YFP-β-catenin dynamics in response to LiCl. HEK293 CCND1-MS2 cells stably expressing YFP-β-catenin were treated with LiCl and increased accumulation of the protein was observed. The YFP signal is

pseudo-colored using ImageJ ''Green Fire Blue' look-up table to show YFP-β-catenin levels. Cells were imaged every 15 min for 825 min.

Video 5. YFP-β-catenin dynamics following Wnt3a activation during cell division. HEK293 CCND1-MS2 cells stably expressing YFP-β-catenin were treated with Wnt3a, and the dynamics of the protein in the nucleus were followed over time. Two cells that undergo mitosis were observed in the field. The levels of the protein in the daughter cells formed from the upper cell were low (also note the appearance and division of the centrosome detected via YFP-β-catenin). In comparison, in the bottom mitotic cell, one daughter cell accumulated high YFP-β-catenin levels very rapidly, while the other responded slowly and had very low levels. The YFP signal is pseudo-colored using ImageJ 'Fire' look-up table to show YFP-β-catenin levels. Cells were imaged every 15 min for 225 min.

Video 6. YFP-β-catenin dynamics following Wnt3a activation during the cell cycle. HEK293 CCND1-MS2 cells stably expressing YFP-β-catenin (yellow) and the Fucci markers for G1 (red) and G2 (cyan), were treated with Wnt3a, and the dynamics of the protein were followed over time.

Video 7. YFP-β-catenin dynamics following Wnt3a activation during cell division. HEK293 CCND1-MS2 cells stably expressing YFP-β-catenin (yellow) and the Fucci markers for G1 (red) and G2 (cyan), were treated with Wnt3a, and the dynamics of the protein were followed over time in four cells that undergo mitosis.

Video 8. YFP-β-catenin dynamics at the cell membrane following Wnt3a activation. HEK293 CCND1-MS2 cells stably expressing YFP-β-catenin were treated with Wnt3a, and the dynamics of the protein at the membrane were followed over time, and were similar to the nucleus and cytoplasm accumulation. The YFP signal is pseudo-colored using ImageJ ''Green Fire Blue' look-up table to show YFP-β-catenin levels. Cells were imaged every 15 min for 1065 min.

Video 9. YFP-β-catenin accumulation at the centrosome following Wnt3a activation. HEK293 CCND1-MS2 cells stably expressing YFP-β-catenin were treated with Wnt3a, and the dynamics of the protein at the centrosome were observed in parallel to the accumulation in the nucleus and cytoplasm. The separation of the centrosome in a cell during division can be seen after the 960 time point. Cells were imaged every 15 min for 1005 min.

Video 10. YFP-β-catenin puncta move from the membrane to the centrosome. HEK293 CCND1-MS2 cells stably expressing YFP-β-catenin were treated with Wnt3a. At the 300 min time point, a series of YFP-β-catenin puncta can be tracked (track colors) moving from the membrane to the centrosome. An inverted presentation of the movie shows the movie puncta (black dots). Cell was imaged every 15 min for 1005 min.

Video 11. YFP-β-catenin puncta move from the membrane to the centrosome. HEK293 CCND1-MS2 cells stably expressing YFP-β-catenin were treated with Wnt3a and MG132. At the 165 min time point, a series of YFP-β-catenin puncta can be tracked (track colors) moving from the membrane to the centrosome. The YFP

signal is pseudo-colored using ImageJ ''Green Fire Blue' look-up table to show YFP-β-catenin levels. Cells were imaged every 15 min for 1065 min.

Video 12. Prolonged activation of CCND1 after Wnt activation. HEK293 CCND1-MS2 cells stably expressing MS2-GFP (green) were treated with Wnt3a. CCND1 mRNA transcription could be detected 15 min after Wnt3a (green dot, transcription site) and continued for 4 hrs. Cells were imaged every 15 min for 270 min.

Figure 1

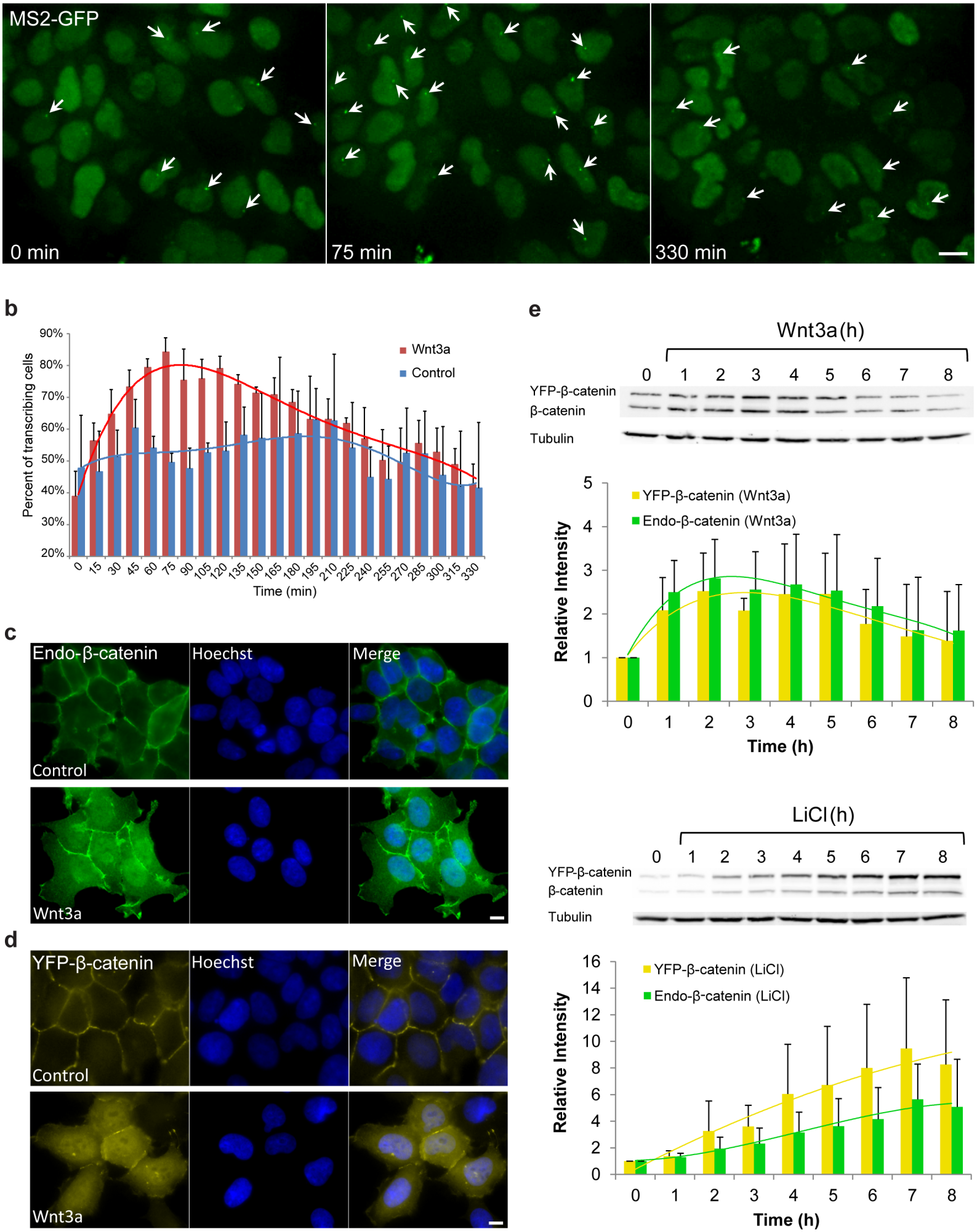
a
MS2-GFP
0 min
75 min
330 min
b
Percent of transcribing cells
Wnt3a
Control
Time (min)
c
Endo-β-catenin
Hoechst
Merge
Control
Wnt3a
d
YFP-β-catenin
Hoechst
Merge
Control
Wnt3a
e
Wnt3a(h)
YFP-β-catenin
β-catenin
Tubulin
YFP-β-catenin (Wnt3a)
Endo-β-catenin (Wnt3a)
Relative Intensity
Time (h)
LiCl(h)
YFP-β-catenin
β-catenin
Tubulin
YFP-β-catenin (LiCl)
Endo-β-catenin (LiCl)
Relative Intensity
Time (h)

Figure 2

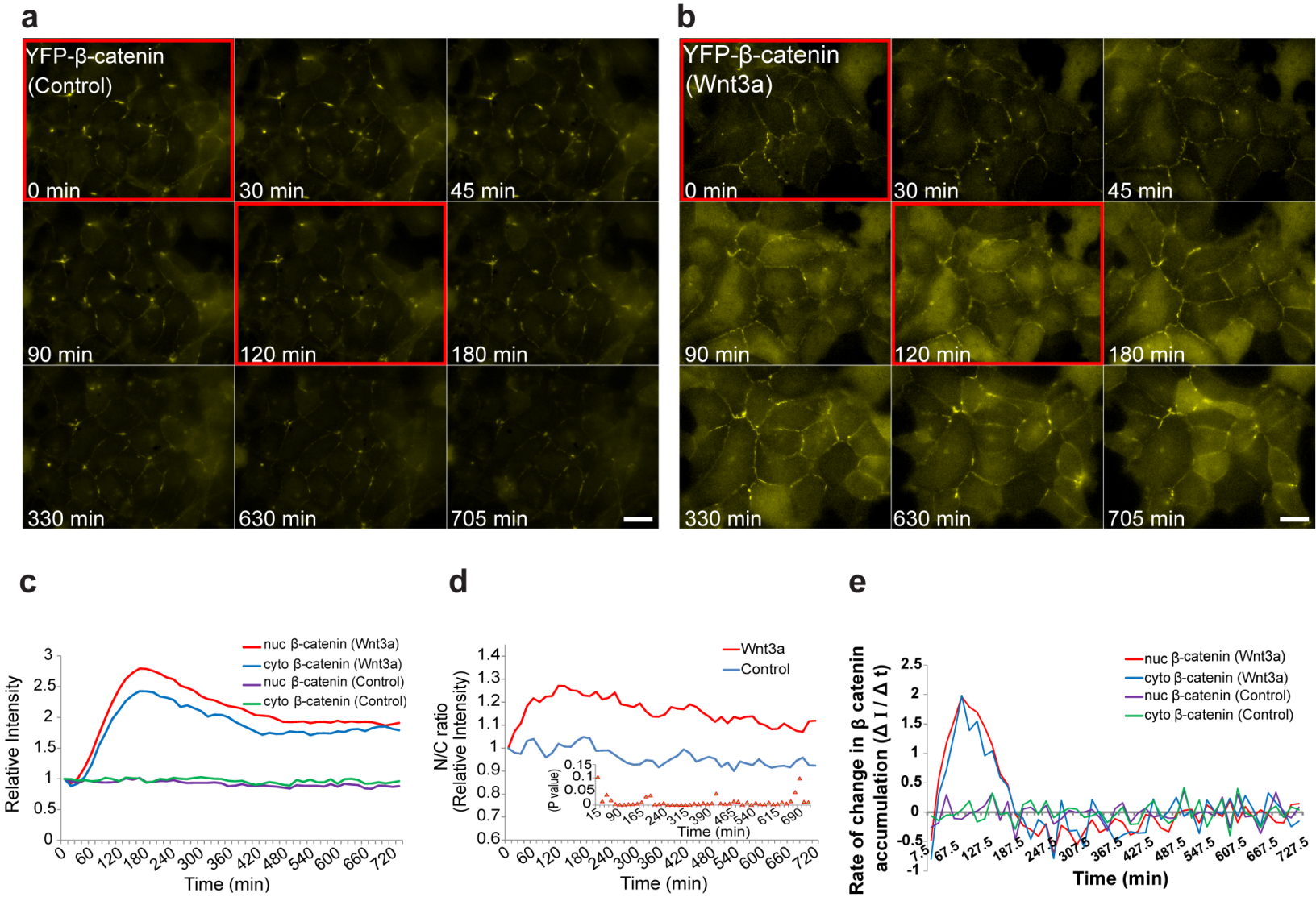
a
YFP-β-catenin
(Control)
0 min
30 min
45 min
90 min
120 min
180 min
330 min
630 min
705 min
b
YFP-β-catenin
(Wnt3a)
0 min
30 min
45 min
90 min
120 min
180 min
330 min
630 min
705 min

c
nuc β-catenin (Wnt3a)
cyto β-catenin (Wnt3a)
nuc β-catenin (Control)
cyto β-catenin (Control)
Relative Intensity
Time (min)

d
Wnt3a
Control
N/C ratio
(Relative Intensity)
(P value)
Time (min)

e
nuc β-catenin (Wnt3a)
cyto β-catenin (Wnt3a)
nuc β-catenin (Control)
cyto β-catenin (Control)
Rate of change in β catenin
accumulation (Δ I / Δ t)
Time (min)

Figure 3

a

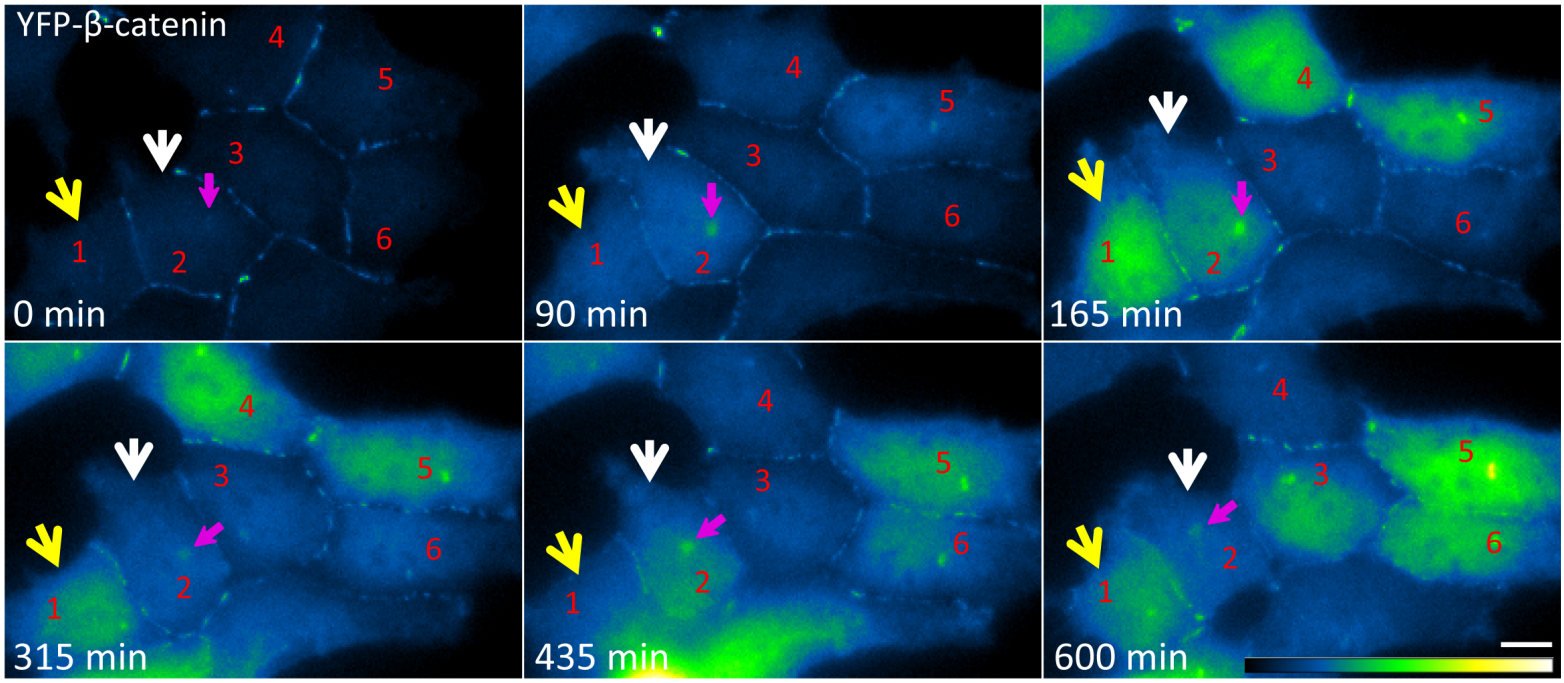
YFP-β-catenin
0 min
90 min
165 min
315 min
435 min
600 min
1
2
3
4
5
6

b

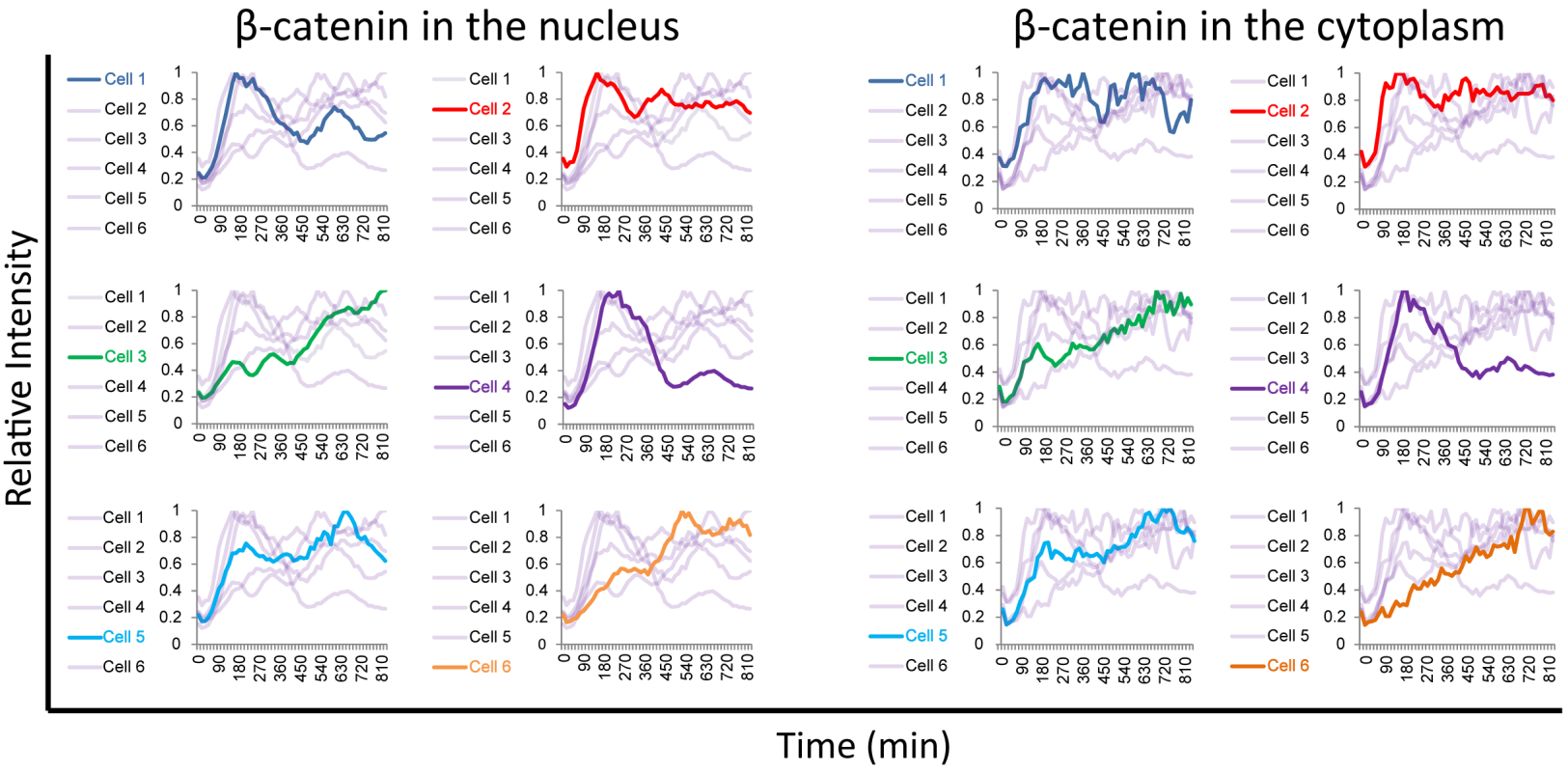
β-catenin in the nucleus
β-catenin in the cytoplasm
Relative Intensity
Time (min)
Cell 1
Cell 2
Cell 3
Cell 4
Cell 5
Cell 6

Figure 4

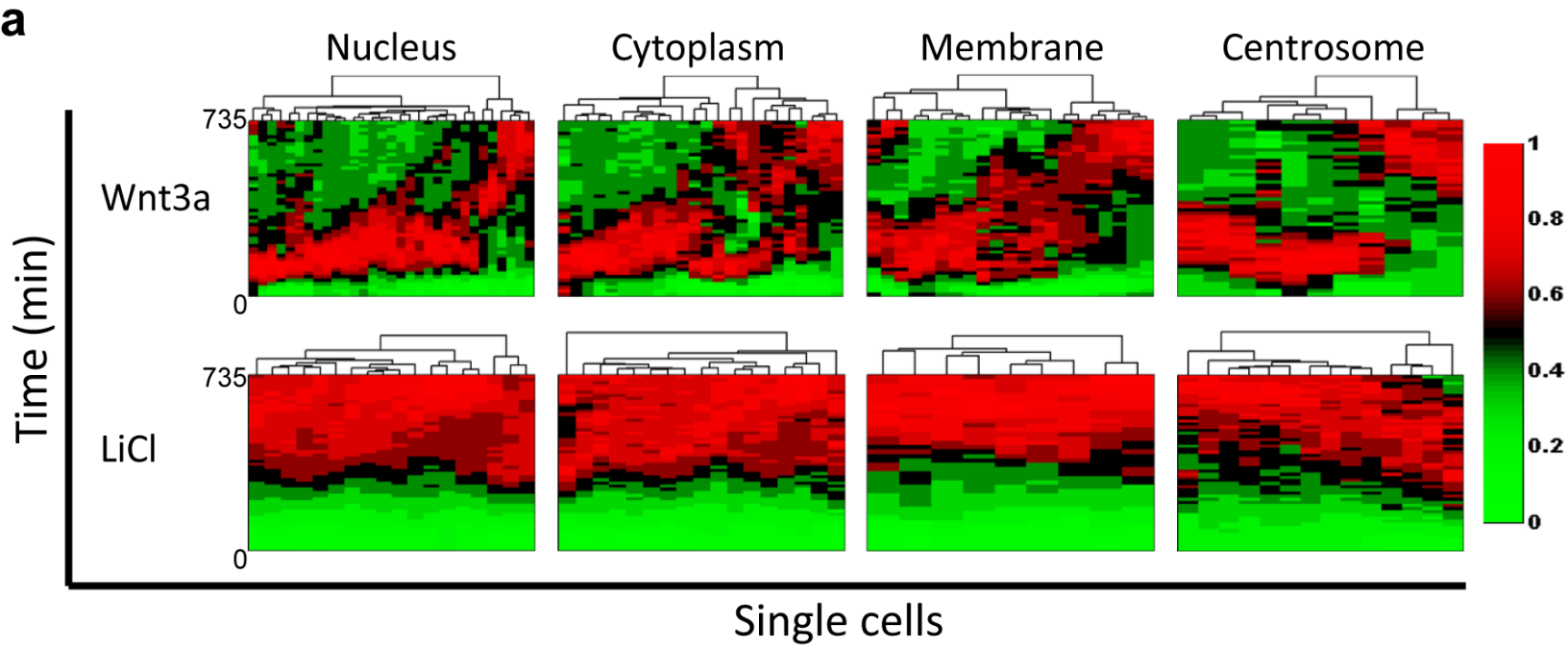
a
Nucleus
Cytoplasm
Membrane
Centrosome
Wnt3a
LiCl
735
0
Time (min)
Single cells
1
0.8
0.6
0.4
0.2
0

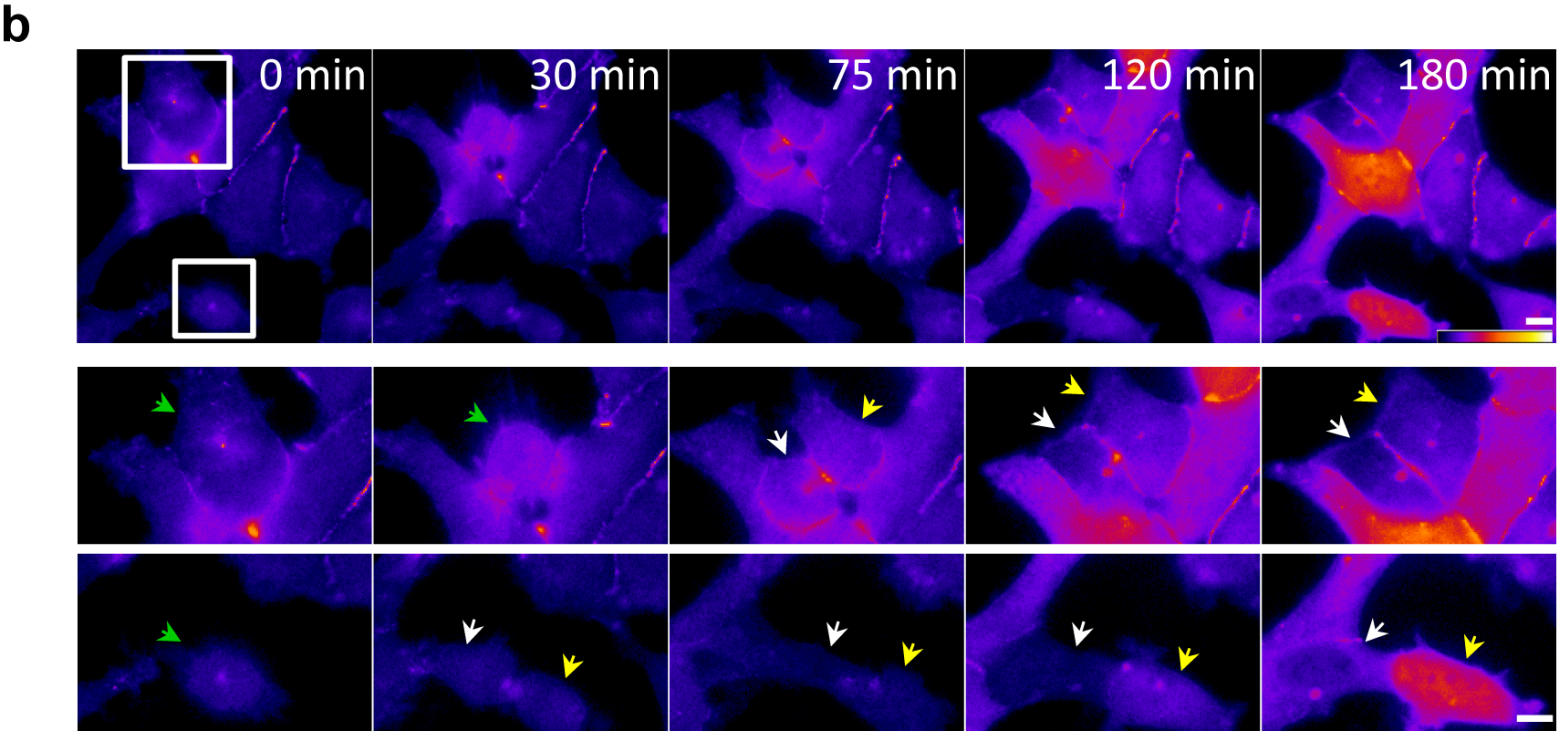
b
0 min
30 min
75 min
120 min
180 min

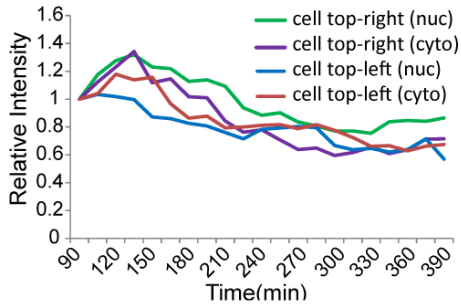
c
Relative Intensity
Time(min)
cell top-right (nuc)
cell top-right (cyto)
cell top-left (nuc)
cell top-left (cyto)

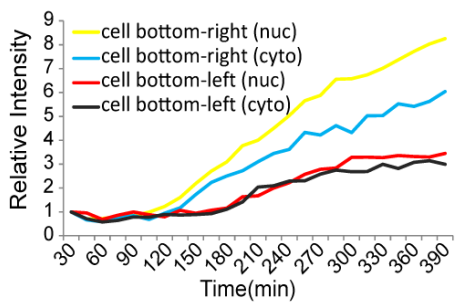
d
Relative Intensity
Time(min)
cell bottom-right (nuc)
cell bottom-right (cyto)
cell bottom-left (nuc)
cell bottom-left (cyto)

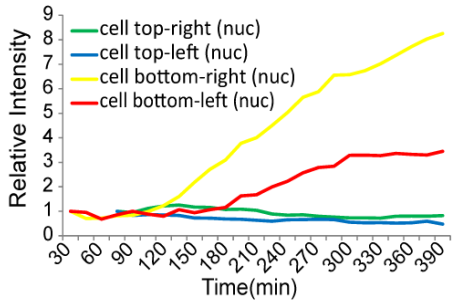
e
Relative Intensity
Time(min)
cell top-right (nuc)
cell top-left (nuc)
cell bottom-right (nuc)
cell bottom-left (nuc)

Figure 5

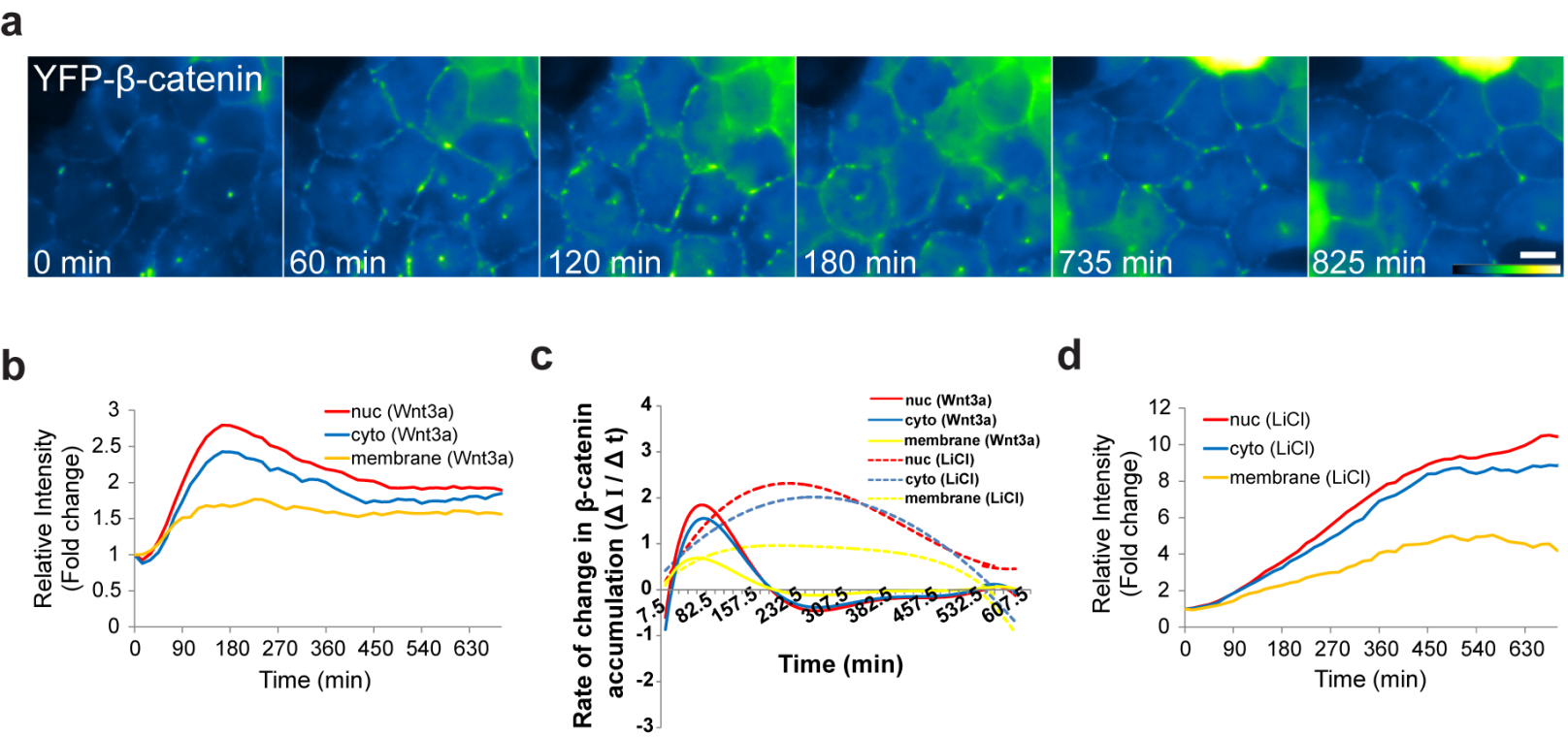
a
YFP-β-catenin
0 min
60 min
120 min
180 min
735 min
825 min
b
Relative Intensity (Fold change)
nuc (Wnt3a)
cyto (Wnt3a)
membrane (Wnt3a)
Time (min)
c
Rate of change in β-catenin accumulation (Δ I / Δ t)
nuc (Wnt3a)
cyto (Wnt3a)
membrane (Wnt3a)
nuc (LiCl)
cyto (LiCl)
membrane (LiCl)
Time (min)
d
Relative Intensity (Fold change)
nuc (LiCl)
cyto (LiCl)
membrane (LiCl)
Time (min)

Figure 6

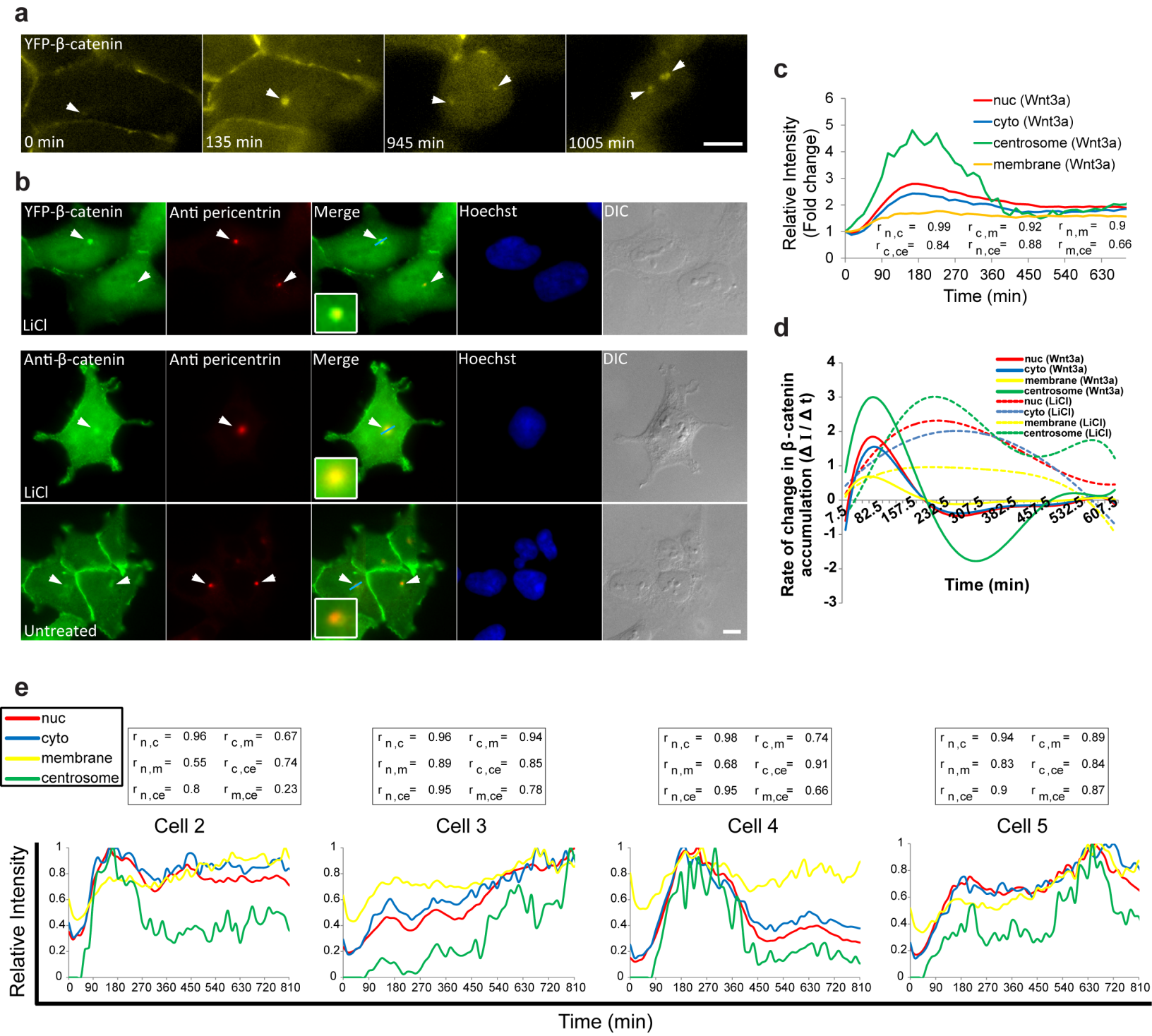
a
YFP-β-catenin
0 min
135 min
945 min
1005 min
b
YFP-β-catenin
Anti pericentrin
Merge
Hoechst
DIC
LiCl
Anti-β-catenin
Anti pericentrin
Merge
Hoechst
DIC
LiCl
Untreated
c
nuc (Wnt3a)
cyto (Wnt3a)
centrosome (Wnt3a)
membrane (Wnt3a)
Relative Intensity (Fold change)
r n,c = 0.99 r c,m = 0.92 r n,m = 0.9
r c,ce = 0.84 r n,ce = 0.88 r m,ce = 0.66
Time (min)
d
nuc (Wnt3a)
cyto (Wnt3a)
membrane (Wnt3a)
centrosome (Wnt3a)
nuc (LiCl)
cyto (LiCl)
membrane (LiCl)
centrosome (LiCl)
Rate of change in β-catenin accumulation (Δ I / Δ t)
Time (min)
e
nuc
cyto
membrane
centrosome
r n,c = 0.96 r c,m = 0.67
r n,m = 0.55 r c,ce = 0.74
r n,ce = 0.8 r m,ce = 0.23
r n,c = 0.96 r c,m = 0.94
r n,m = 0.89 r c,ce = 0.85
r n,ce = 0.95 r m,ce = 0.78
r n,c = 0.98 r c,m = 0.74
r n,m = 0.68 r c,ce = 0.91
r n,ce = 0.95 r m,ce = 0.66
r n,c = 0.94 r c,m = 0.89
r n,m = 0.83 r c,ce = 0.84
r n,ce = 0.9 r m,ce = 0.87
Cell 2
Cell 3
Cell 4
Cell 5
Relative Intensity
Time (min)

Figure 7

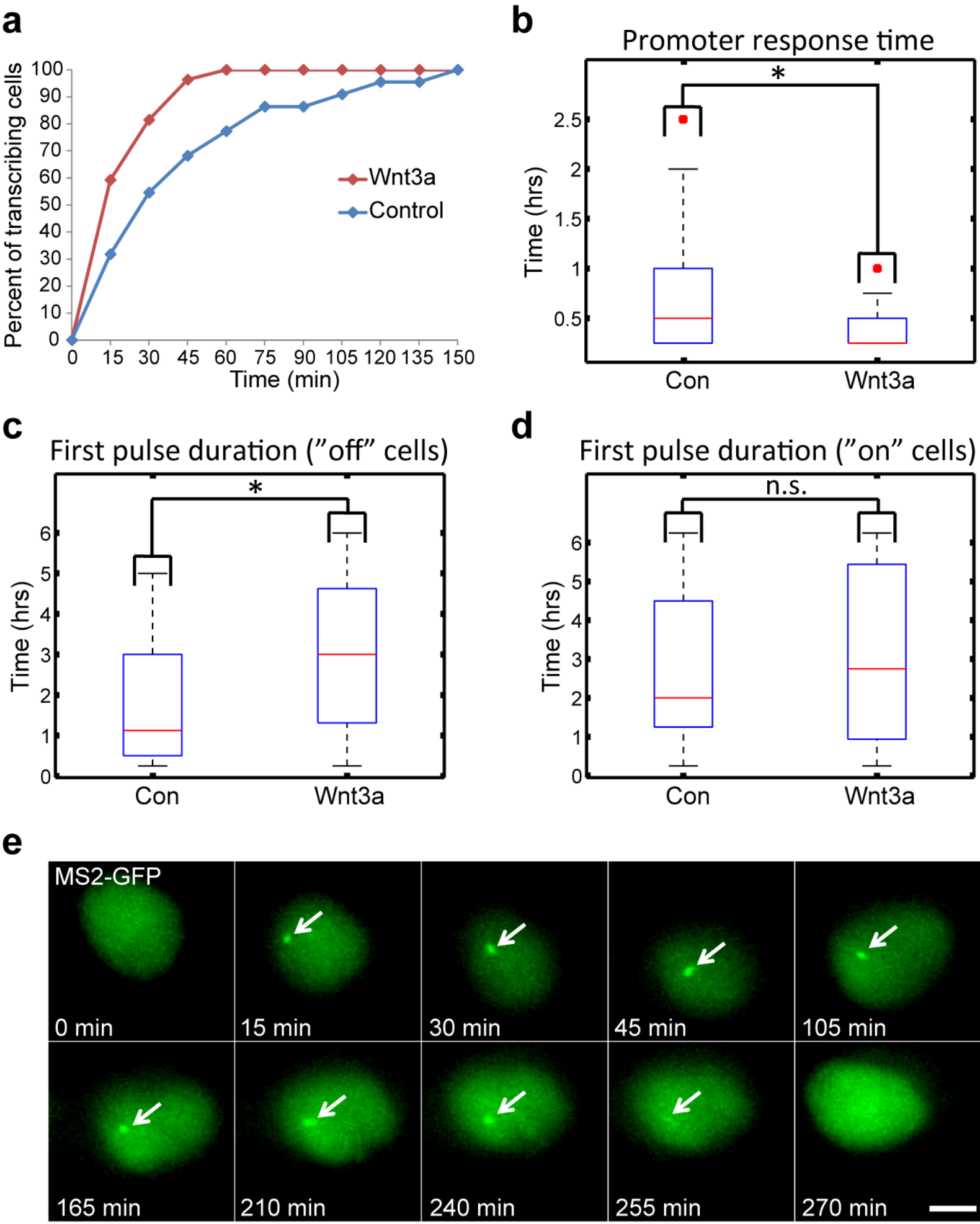
a
Percent of transcribing cells
100
90
80
70
60
50
40
30
20
10
0
0 15 30 45 60 75 90 105 120 135 150
Time (min)
Wnt3a
Control
b
Promoter response time
*
Time (hrs)
2.5
2
1.5
1
0.5
Con
Wnt3a
c
First pulse duration (”off” cells)
*
Time (hrs)
6
5
4
3
2
1
0
Con
Wnt3a
d
First pulse duration (”on” cells)
n.s.
Time (hrs)
6
5
4
3
2
1
0
Con
Wnt3a
e
MS2-GFP
0 min
15 min
30 min
45 min
105 min
165 min
210 min
240 min
255 min
270 min

Figure 8

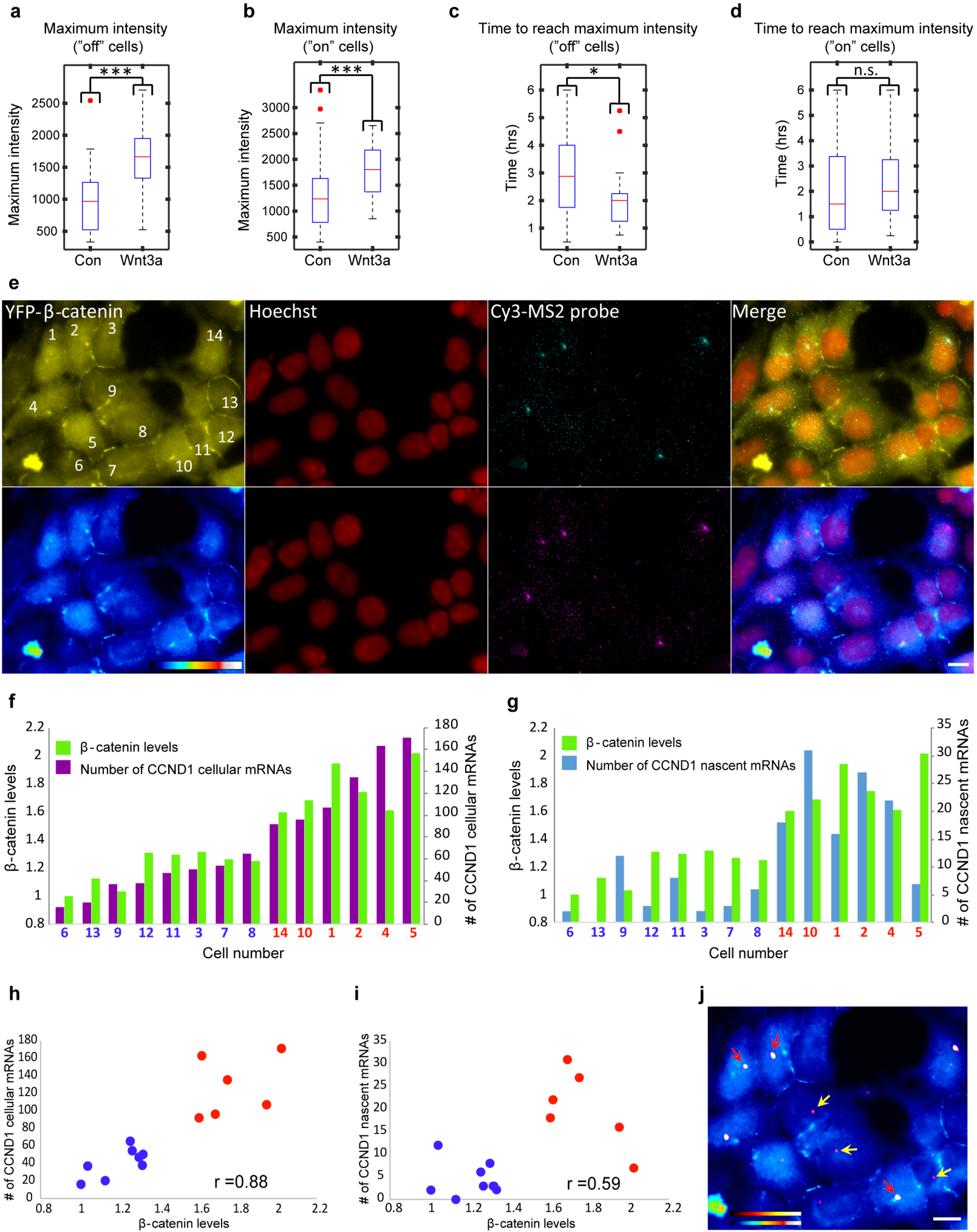
a
Maximum intensity
("off" cells)
***
Maximum intensity
2500
2000
1500
1000
500
Con
Wnt3a
b
Maximum intensity
("on" cells)
***
Maximum intensity
3000
2500
2000
1500
1000
500
Con
Wnt3a
c
Time to reach maximum intensity
("off" cells)
*
Time (hrs)
6
5
4
3
2
1
Con
Wnt3a
d
Time to reach maximum intensity
("on" cells)
n.s.
Time (hrs)
6
5
4
3
2
1
0
Con
Wnt3a
e
YFP-β-catenin
Hoechst
Cy3-MS2 probe
Merge
1
2
3
14
9
4
13
8
5
12
11
6
7
10
f
β-catenin levels
Number of CCND1 cellular mRNAs
β-catenin levels
# of CCND1 cellular mRNAs
2.2
2
1.8
1.6
1.4
1.2
1
0.8
180
160
140
120
100
80
60
40
20
0
6
13
9
12
11
3
7
8
14
10
1
2
4
5
Cell number
g
β-catenin levels
Number of CCND1 nascent mRNAs
β-catenin levels
# of CCND1 nascent mRNAs
2.2
2
1.8
1.6
1.4
1.2
1
0.8
35
30
25
20
15
10
5
0
6
13
9
12
11
3
7
8
14
10
1
2
4
5
Cell number
h
# of CCND1 cellular mRNAs
180
160
140
120
100
80
60
40
20
0
r =0.88
0.8
1
1.2
1.4
1.6
1.8
2
2.2
β-catenin levels
i
# of CCND1 nascent mRNAs
35
30
25
20
15
10
5
0
r =0.59
0.8
1
1.2
1.4
1.6
1.8
2
2.2
β-catenin levels
j

Figure 9

a

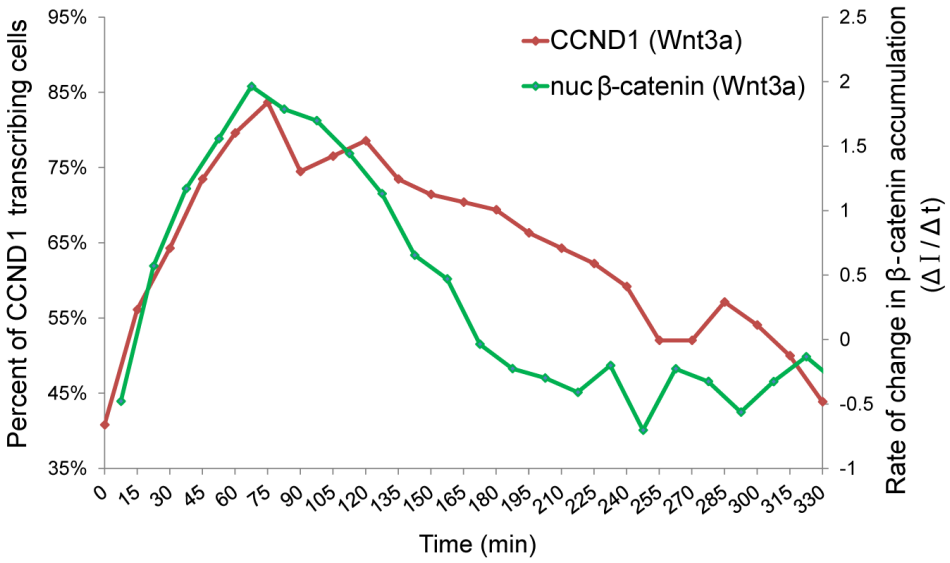
CCND1 (Wnt3a)
nuc β-catenin (Wnt3a)
Percent of CCND1 transcribing cells
Rate of change in β-catenin accumulation (Δ I / Δ t)
Time (min)
95%
85%
75%
65%
55%
45%
35%
2.5
2
1.5
1
0.5
0
-0.5
-1
0 15 30 45 60 75 90 105 120 135 150 165 180 195 210 225 240 255 270 285 300 315 330

b

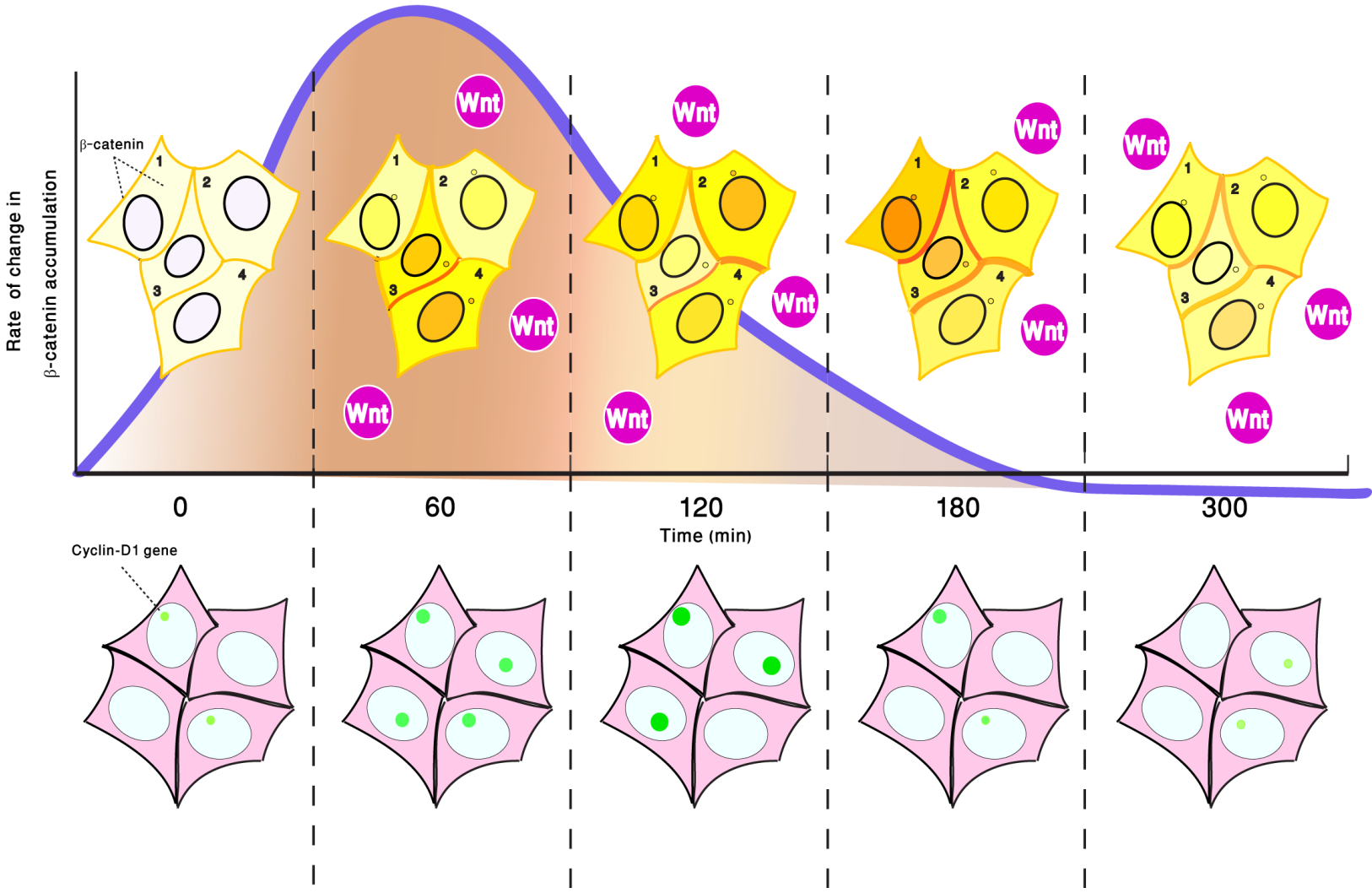
Rate of change in β-catenin accumulation
β-catenin
Wnt
0
60
120
180
300
Time (min)
Cyclin-D1 gene

Figure 1-figure supplement 1

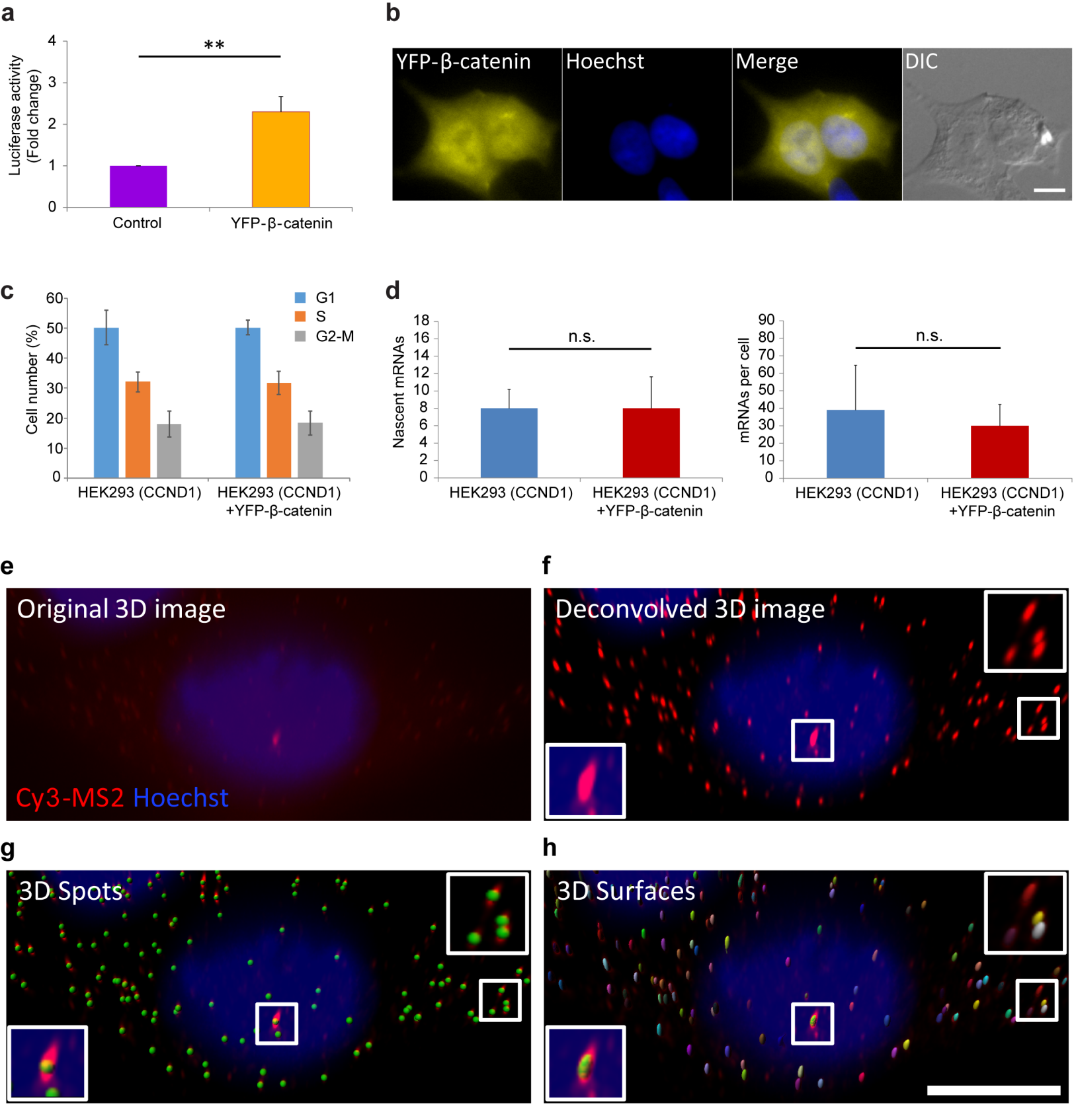

Figure 2-figure supplement 1

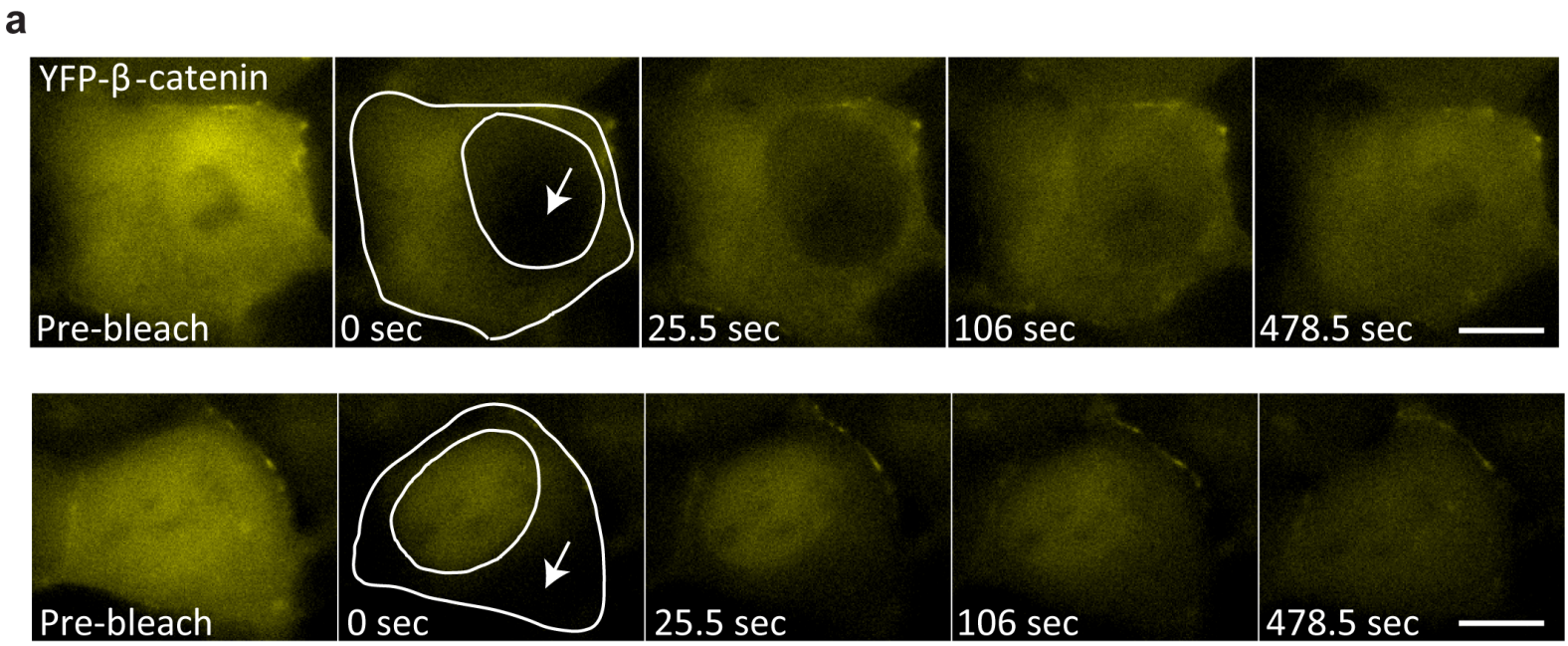

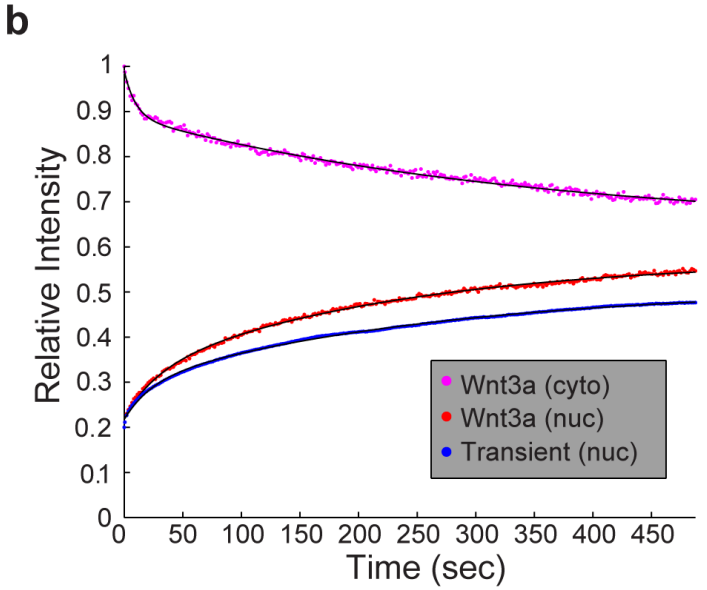

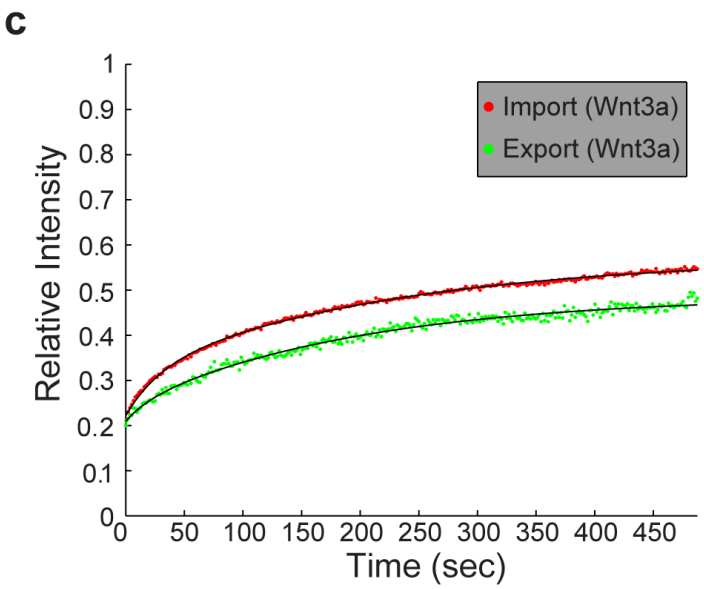

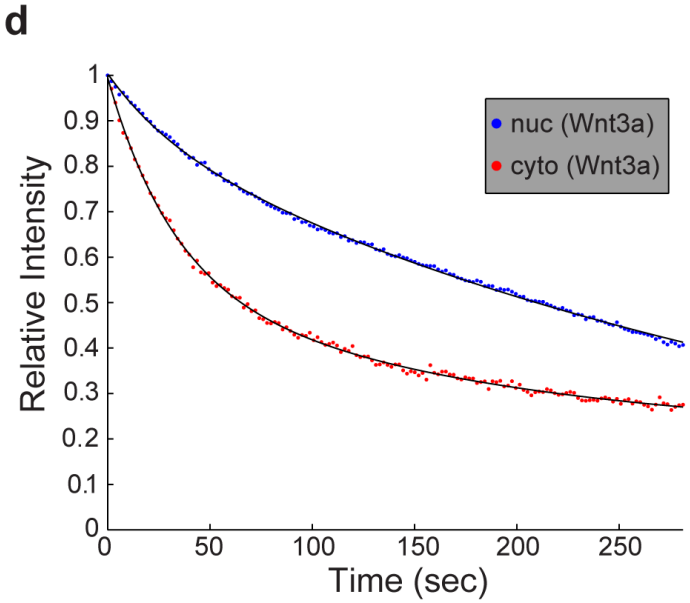

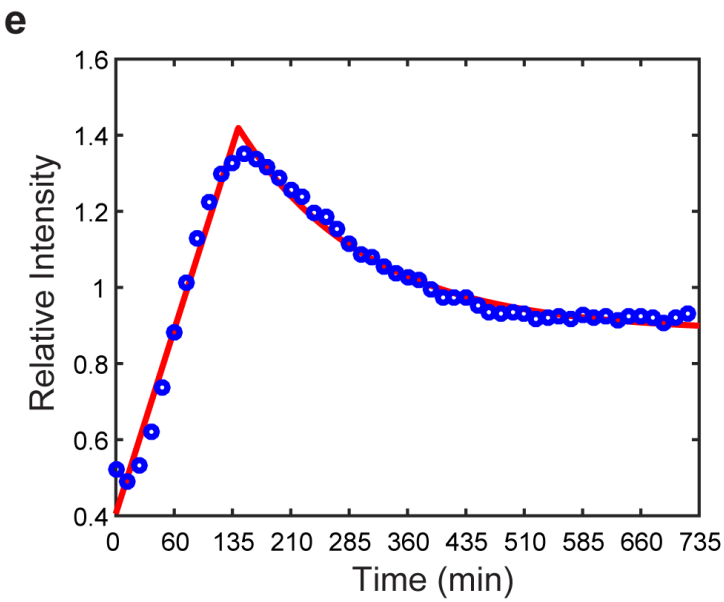

Figure 3-figure supplement 1

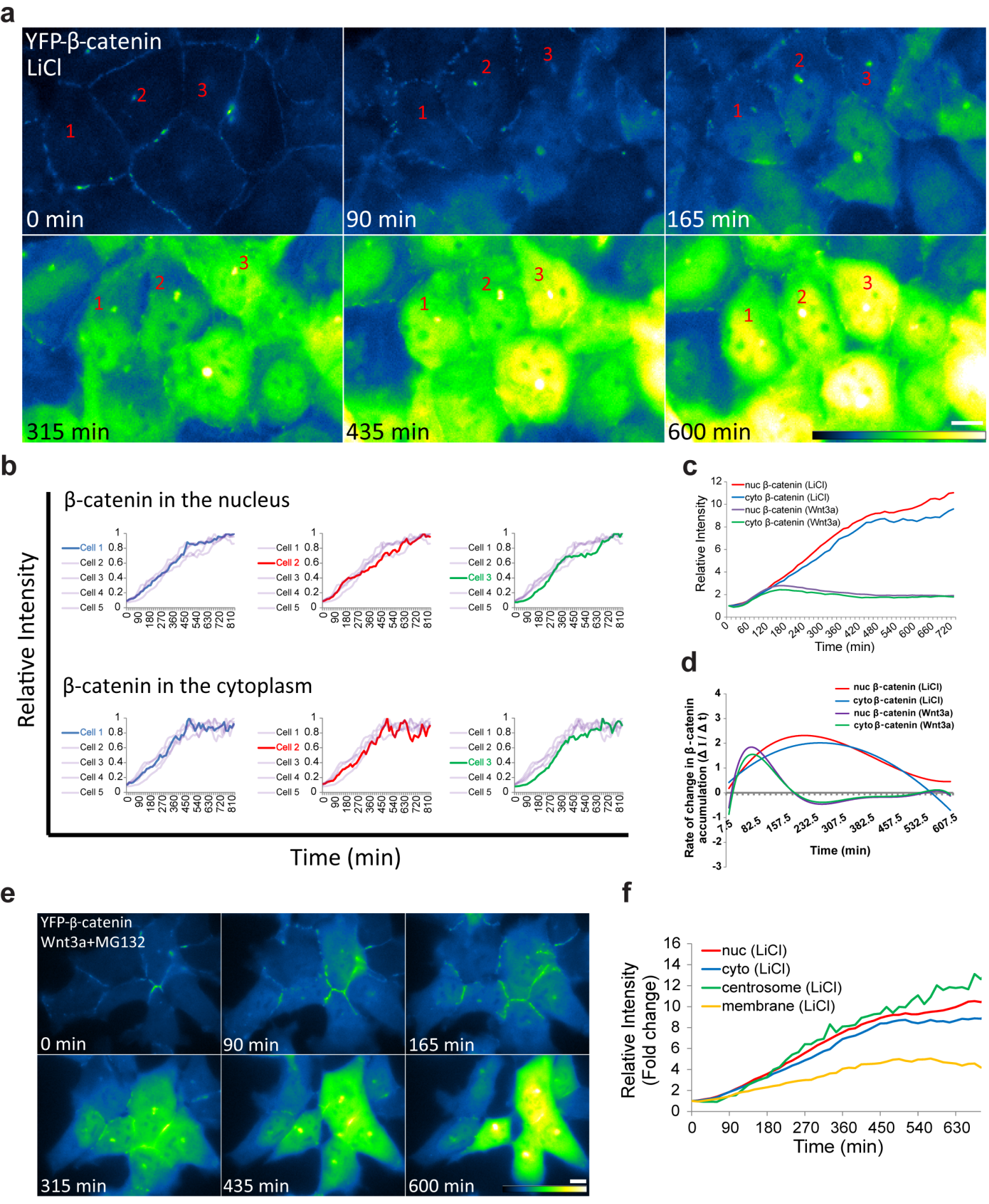

Figure 3-figure supplement 2

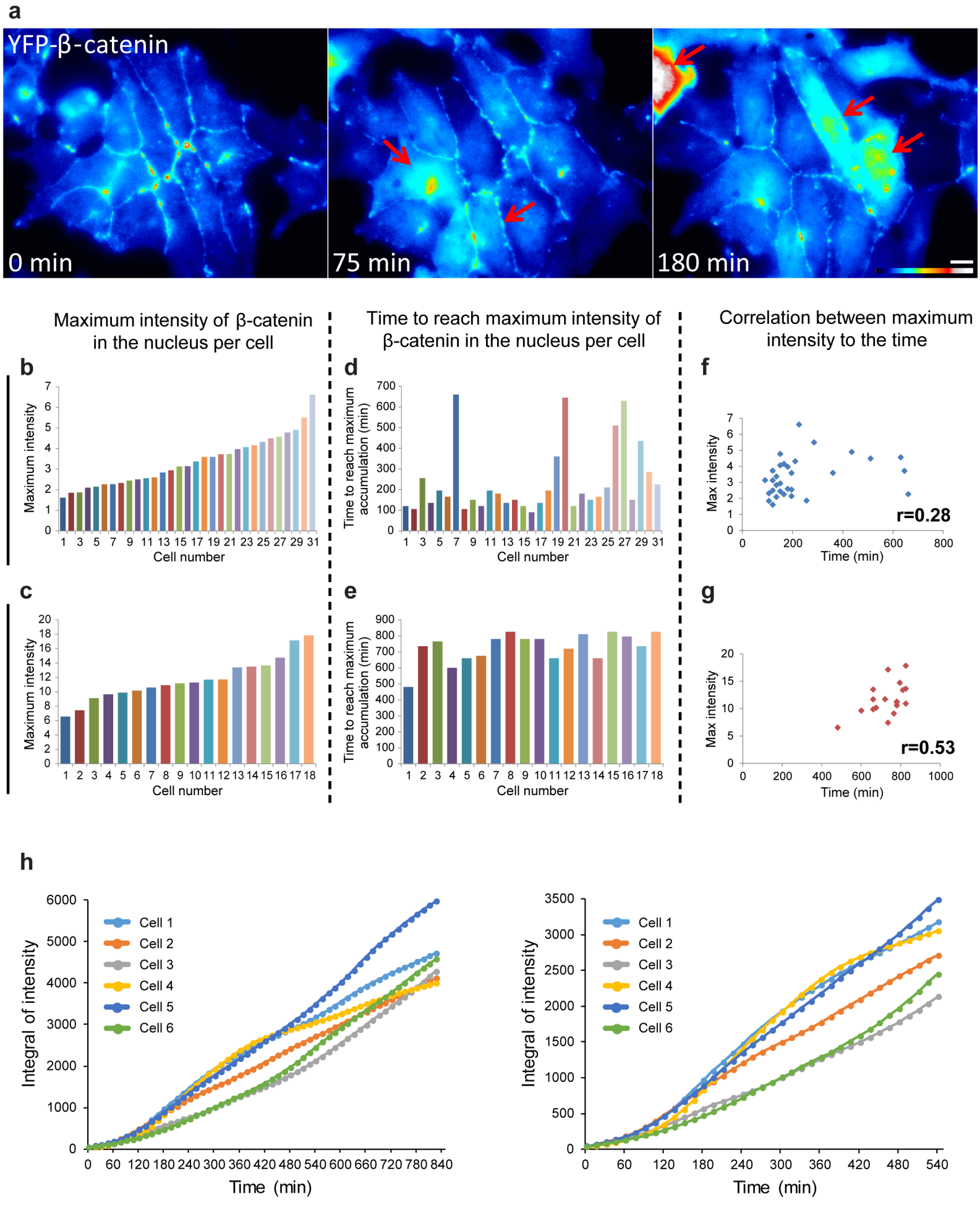

Figure 4-figure supplement 1

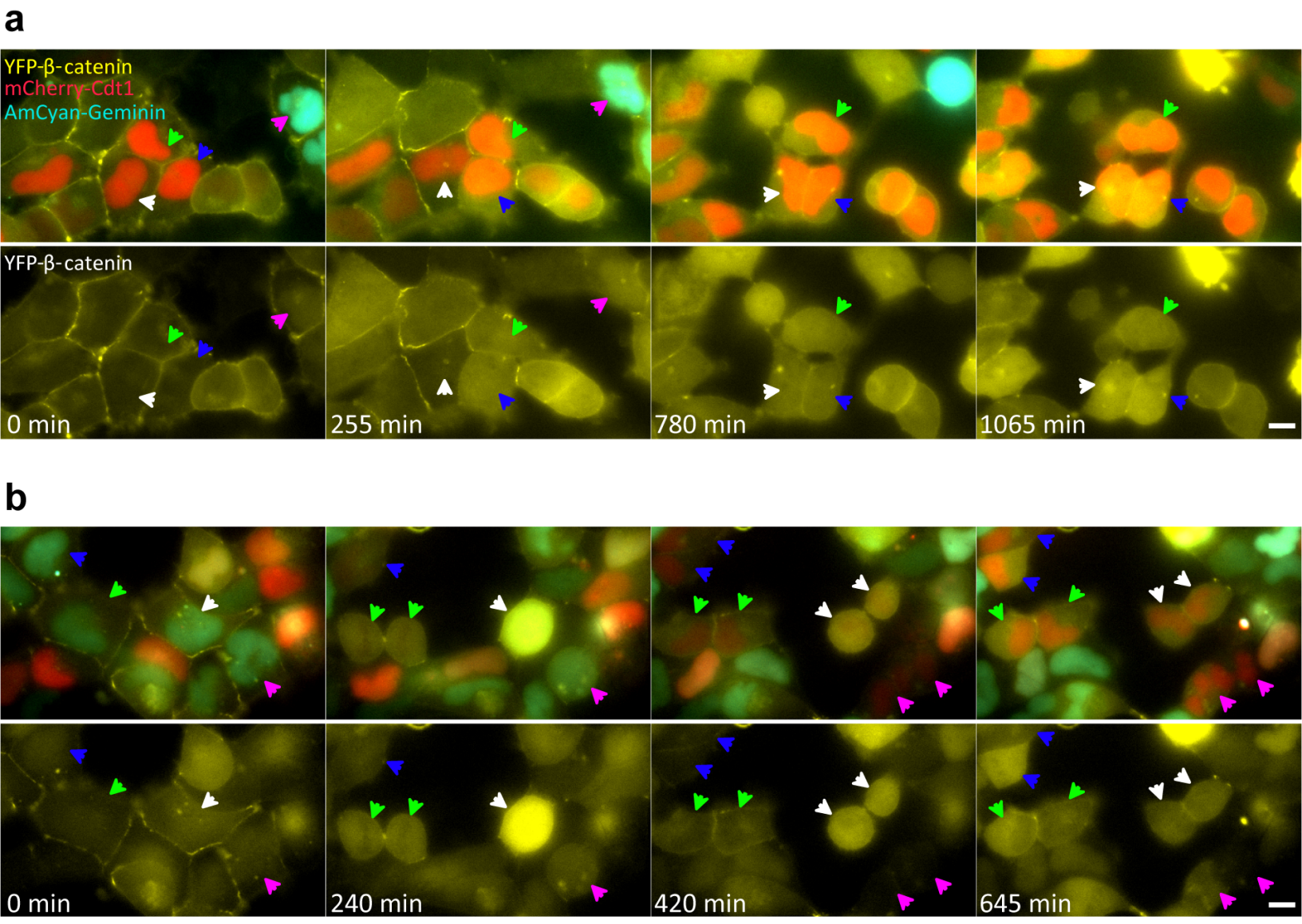

Figure 5-figure supplement 1

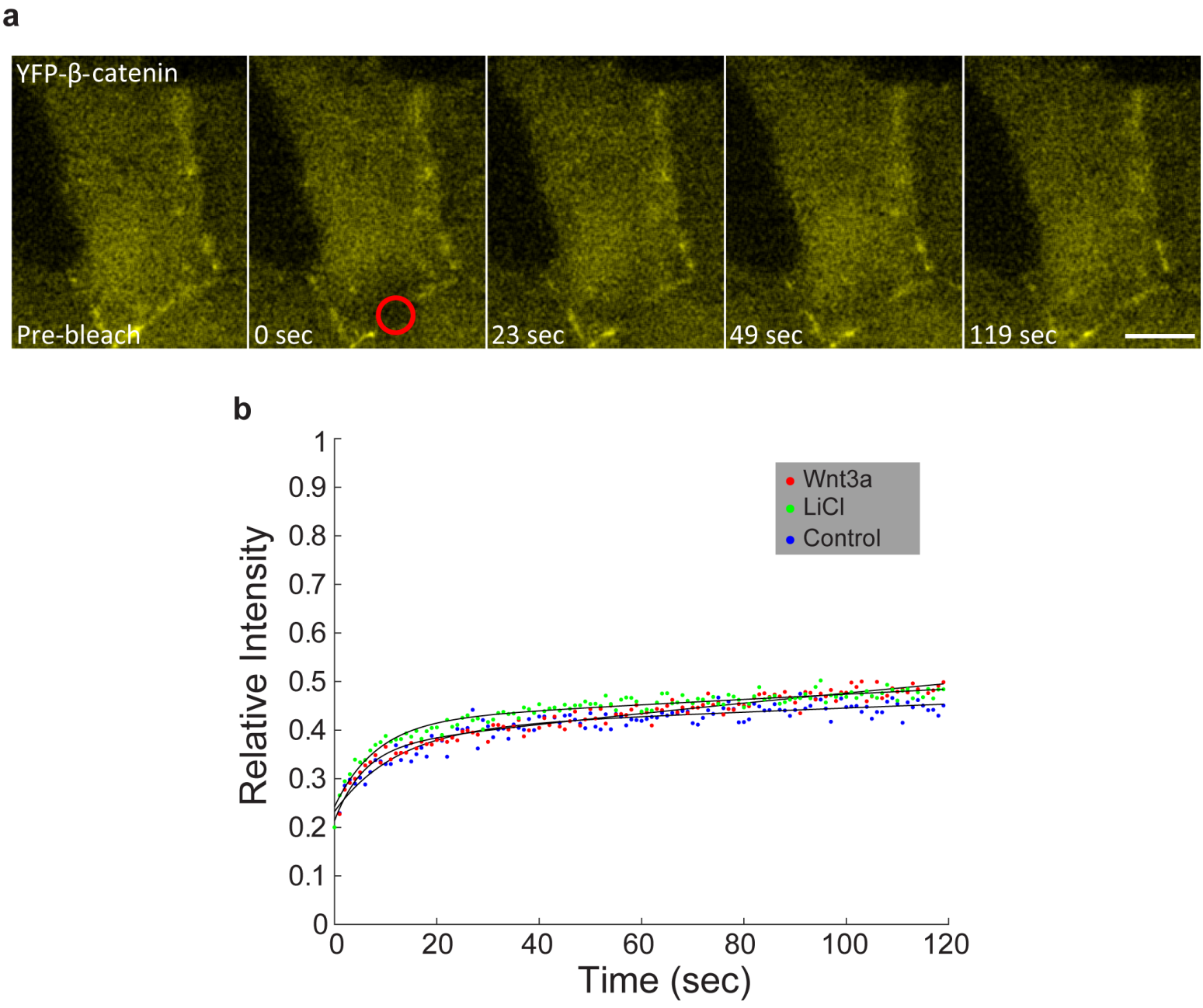

Figure 6-figure supplement 1

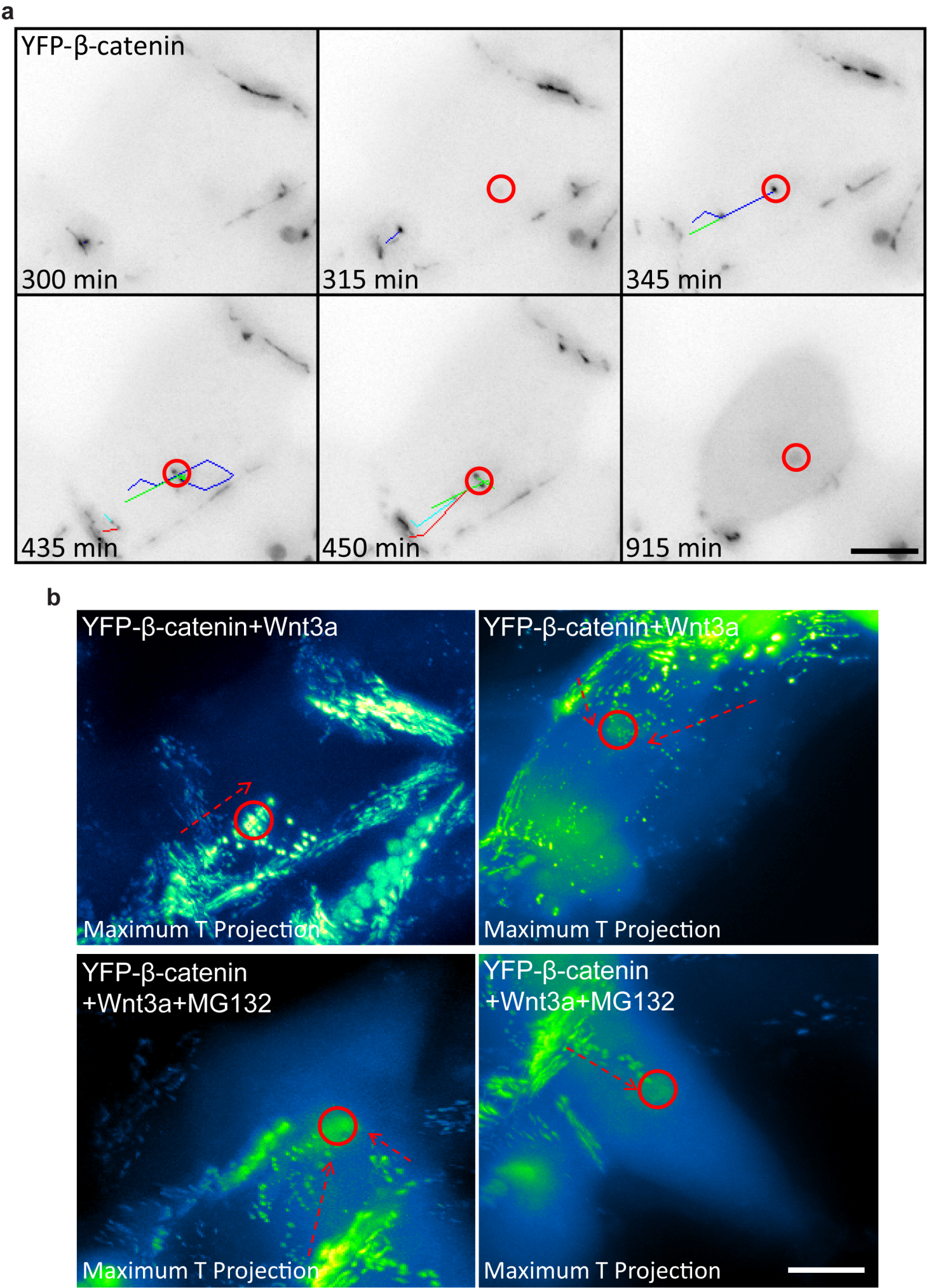

Figure 6-figure supplement 2

a

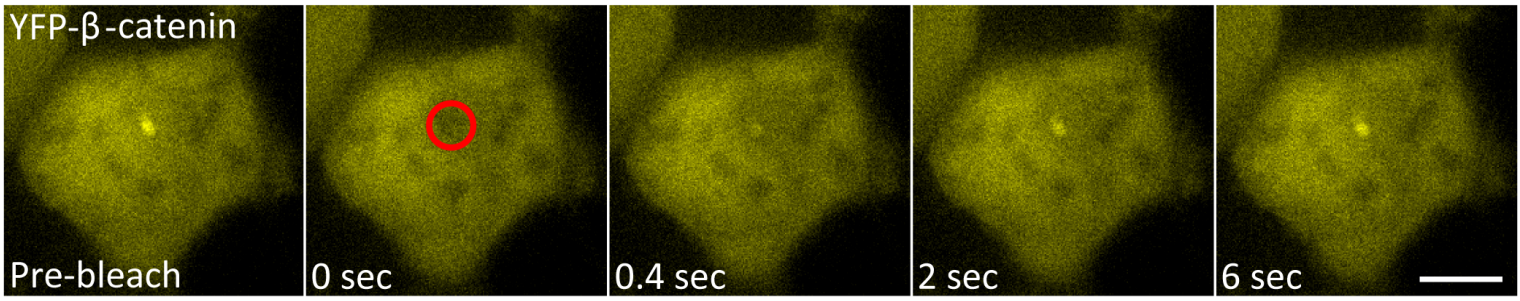

b

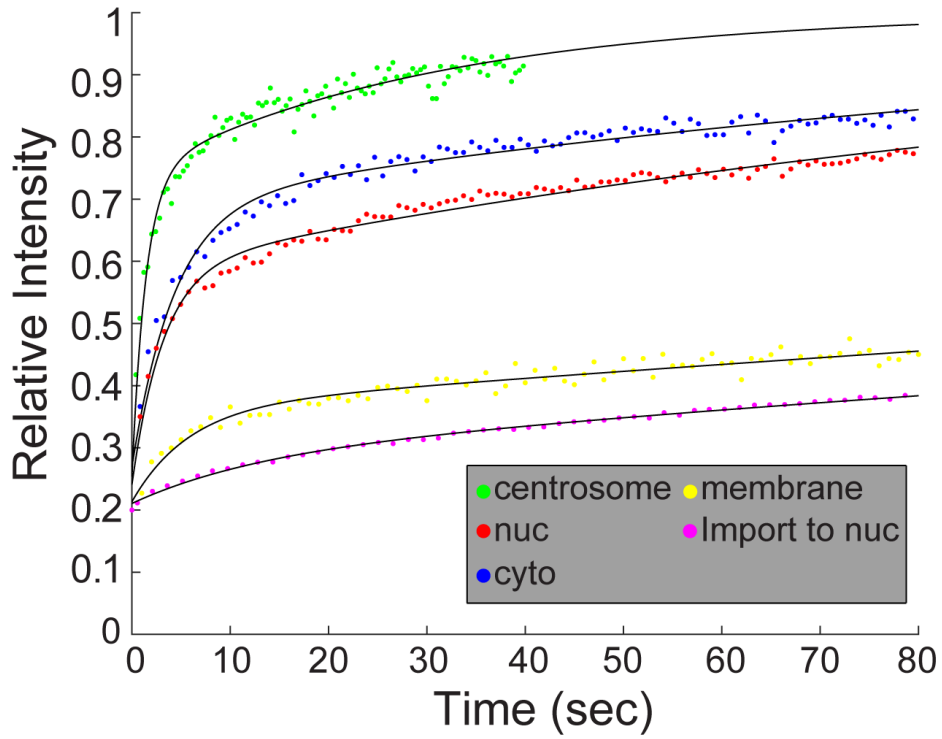

Figure 7-figure supplement 1

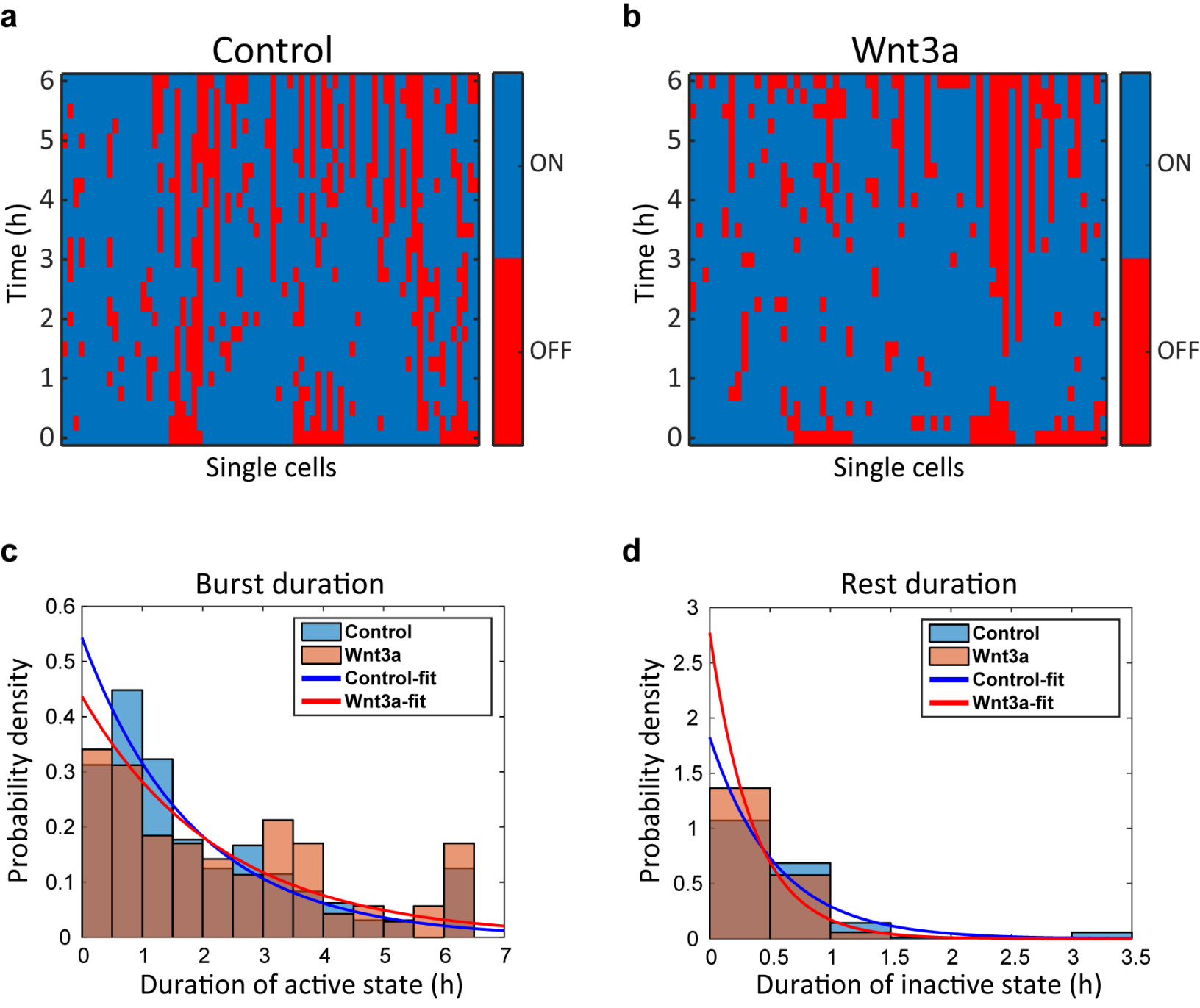

Figure 8-figure supplement 1